CALIFORNIA INSTITUTE OF TECHNOLOGY

BIG BEAR SOLAR OBSERVATORY

HALE OBSERVATORIES

[redacted]

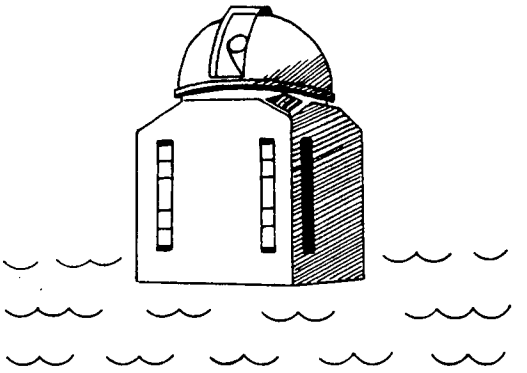

THE FLARES OF AUGUST 1972

by

Harold Zirin and Katsuo Tanaka

BIG BEAR SOLAR OBSERVATORY, HALE OBSERVATORIES

CARNEGIE INSTITUTION OF WASHINGTON

CALIFORNIA INSTITUTE OF TECHNOLOGY

Received_____

BBSO #0128

ABSTRACT

We present the analysis of observations of the August flares at Big Bear and Tel Aviv, involving monochromatic movies, magnetograms and spectra. In each flare the observations fit a model of particle acceleration in the chromosphere with emission produced by impart and by heating by the energetic electrons and protons. The region showed twisted flux and high gradients from birth, and flares appear due to strong magnetic shears and gradients across the neutral line produced by sunspot motions. Post flare loops show a strong change from sheared, force-free fields parallel to potential-field-like loops, perpendicular to the neutral line above the surface.

We detected fast (10 sec duration) small (1 arc sec) flashes in 3835 at the footpoints flux loops in the August 2 impulsive flare at 1838, which may be explained by dumping of > 50 KeV electrons accelerated in individual flux loops. The flashes show excellent time and intensity agreement with > 45 KeV x-rays. In the less impulsive 20:00 U.T. flare a less impulsive wave of emission in 3835 moved with the separating footpoints. The thick foil model of x-ray production gives a consistent model for x-ray, 3835 and microwave emission in the 1838 event.

Spectra of the August 7 flare show emission 12 Å FWHM in flare kernels, but only 1 to 2 Å wide in the rest of the flare.

The kernels thus produce most of the Hα emission. The total emission in Hα in the August 4 and August 7 flares was about 2×10^{30} ergs. We believe this dependable value more accurate than previous larger estimates for great flares. The time dependence of total Hα emission agrees with radio and x-ray data much better than area measurements which depend on the weaker halo.

Absorption line spectra show a large (6 km/sec) photospheric velocity discontinuity along the neutral line, corresponding to sheared flow across that line.

I. INTRODUCTION

The active region McMath 11976, which produced the great flares of August 1972, produced an unparalleled opportunity for the study of solar activity. We present optical observations made at the Big Bear Solar Observatory and its station at Tel Aviv University, and comparisons with data kindly made available by various colleagues.

The data at Big Bear Lake were made with a battery of telescopes on a single mount. Two 10-inch refractors produced large scale cinematographic data in various wavelengths, mostly Hα and Hα $\pm$ 1/2 Å, but also on August 2 with a Chapman filter (Chapman, 1971) 15 Å wide, centered on 3835 Å. Observations of the full disc in Hα were made with an 8.6-inch vacuum refractor, white light full disc observations with a 6-inch refractor. Magnetograms were made with the Leighton-Smithson magnetograph, time sharing in one of the 10-inch refractors, and spectrograms, with the 5 meter Coude spectrograph fed by a third 10-inch refractor. At Tel Aviv, observations were made with a 5-inch photoheliograph used in the center of Hα. We were fortunate in that not only was the birth of the region observed in July, but all of the large flares were picked up on either the Big Bear or Tel Aviv photoheliographs. The principal large flares occurred at 03:30 August 2 (only observed in progress), 18:38 August 2, 20:05 August 2, 06:20 August 4, 15:16 August 7, and 12:16 August 11 (only late phases).

The highlights of the observations are the following: the region showed inverted polarity from its inception on July 11; the great activity was due to extremely high shear and gradients in the magnetic field, as well as a constant invasion of one polarity into the opposite; observations in 3835 show remarkable fast flashes in the impulsive flare of 18:38 on August 2 with lifetimes of 5 seconds, which may be due to dumping of particles in the lower chromosphere; flare loops show evolutional increases of their tilts to the neutral line in the flares of August 4 and 7; spectroscopic observations show red asymmetry and red shift of the Hα emission in the flash phase of the August 7 flare, as well as substantial velocity shear in the photosphere during the flare, somewhat like earthquake movement along a fault; finally the total Hα emission of the August 7 flare could be measured accurately as about 2.5×10^{30} ergs, considerably less than coarser previous estimates for great flares. A preliminary report on our data has appeared (Tanaka and Zirin, 1973) and we present here our comprehensive analysis of the wealth of material obtained.

II. DEVELOPMENT OF THE REGION, JULY 10 TO 15

McMath 11957, the predecessor of McMath 11976, first appeared on Big Bear films on July 11, growing in a quiet region. Figure 1 shows an Hα picture of development on July 12 and Figure 2, the magnetograms. Contrary to popular belief, such regions do not emerge from the elements of the network but in perfectly quiet regions in between--note the black dot (*p* polarity) in the 10 July magnetogram. The magmetic polarity was inverted from the start, the arched filaments being rotated 120° from the normal E-W direction. In addition to the first set of flux loops, other systems arose, so that on July 12 there were 2 sets of *f* spots, both connected to the same *p* area. Between July 12 and July 13 there was rapid growth of the *p* spot, and the magnetogram for the 13th shows the strong field gradients thus produced. A number of small flares were observed in this region, and spectra were obtained of intense small surges at the limb on the 15th. The limb activity on the 15th was almost continuous, made up of many small surges. It is clear that the magnetic complexity of this region was inherent in its structure from its first emergence from below and was not a consequence of interaction with existing regions. McMath 11947, the region just ahead of it, died out on the back side and was not seen the next time around.

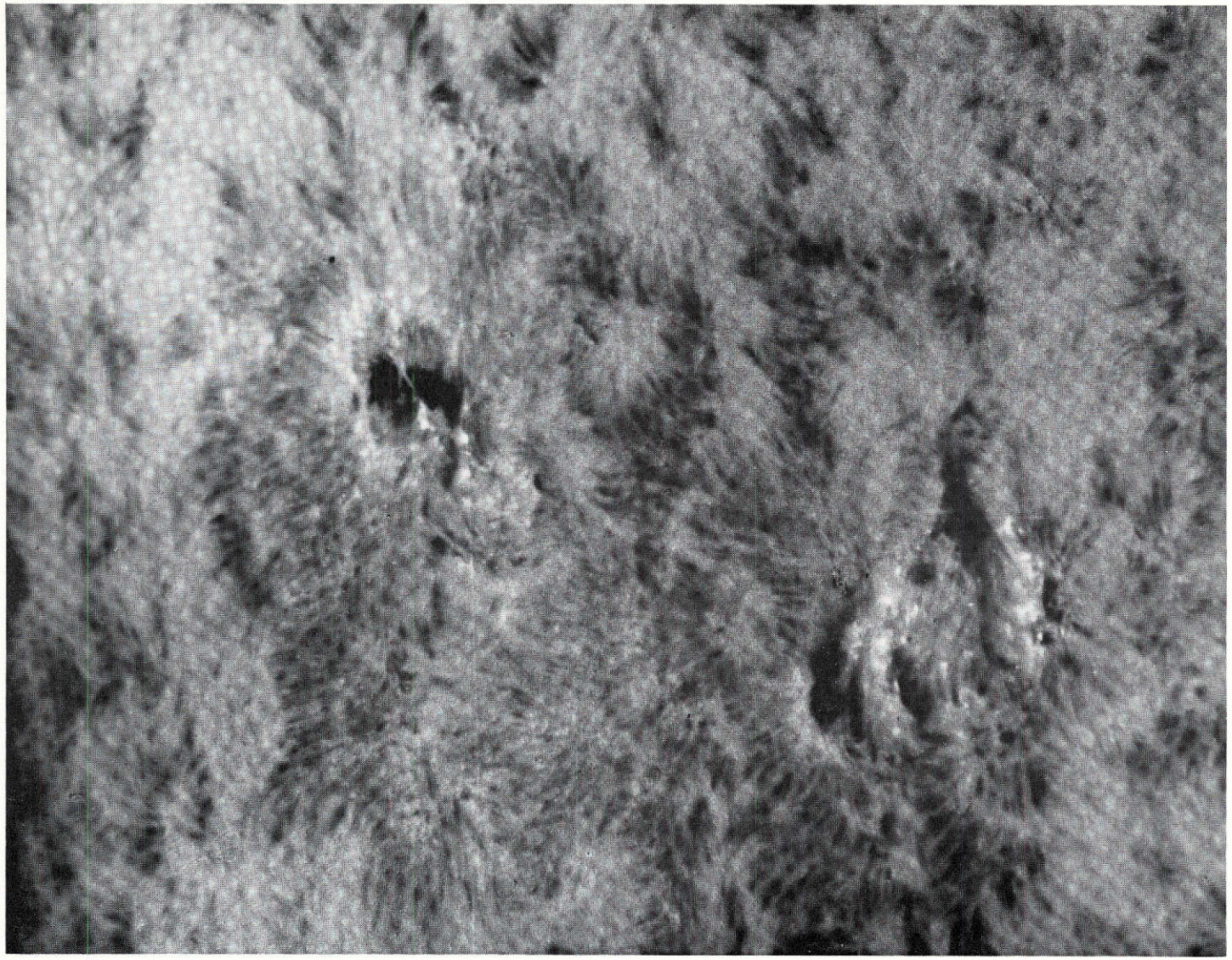

Figure 1

Early stage of McMath 11976 (as McMath 11957) at 18:17:23, July 12, Hα + 0.5 Å. It is in the lower center of the frame, a typical complex emerging flux region (EFR). The dark fibrils probably parallel new flux loops, and would normally run E-W in a simple region. Comparison with Figure 2 shows that the sunspot in the upper part of the group is *p* (preceding, or S) polarity, and the regions below and surrounding are *f* (following, N). The spots at left died out on the back side of the sun. S top, W left on all photos.

6c

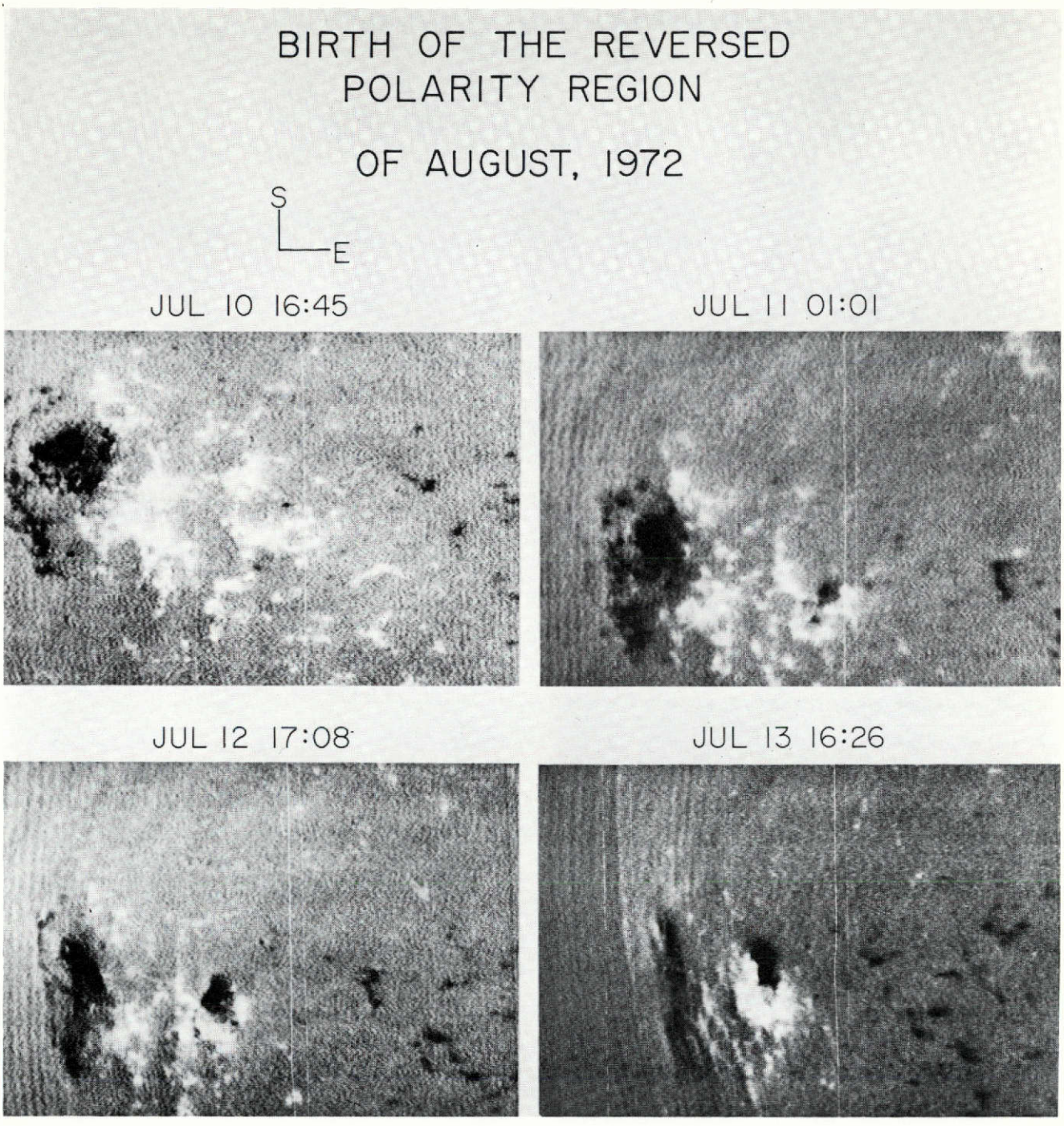

Figure 2

A series of videomagnetograms of the birth of McMath 11957 made by James Mosher. Dark is *p* (preceding, or S in the northern hemisphere this cycle) polarity, white is *f* or following. Note the contrast of the complex new region with the larger old region at left, where dark (*p*) polarity leads, as it normally should.

III. DEVELOPMENT JULY 30 TO AUGUST 2

McMath 11976 appeared at the east limb on July 29, with high resolution observations at Big Bear beginning on the 30th. Although the official prediciton was that "solar activity will remain at a low to moderate level," close inspection of the small region showed a tightly twisted magnetic configuration with steep field gradients and *f* polarity directly S of the main spot. Figures 3, 4 and 5 show the disk transit of the region from July 30 to August 11, and Figure 6 shows the daily magnetograms obtained by James Mosher. The region was only moderately active on the 30th and 31st of July; there were a number of small flares along the neutral line, all fast and impulsive. This neutral line was the dominant feature of the group during its disc passage. It is best seen in Figure 7, which shows an enlarged view of the spot on August 3 in Hα centerline on which we have marked various features. A ragged N-S line of field transition arches (FTA) and longer dark fibrils separates the *f* and *p* polarities. We distinguish these because the FTA in the upper part are short fibrils connecting nearby fields and running more or less perpendicular to the neutral line, whereas the fibrils in the lower (N) half, while physically similar, run, like filaments, parallel to the boundary line and are considerably longer. These long fibrils show the great shear that existed along the neutral line. Eventually the FTA were sheared into filaments, and filament 1 extended, with a few breaks, all the

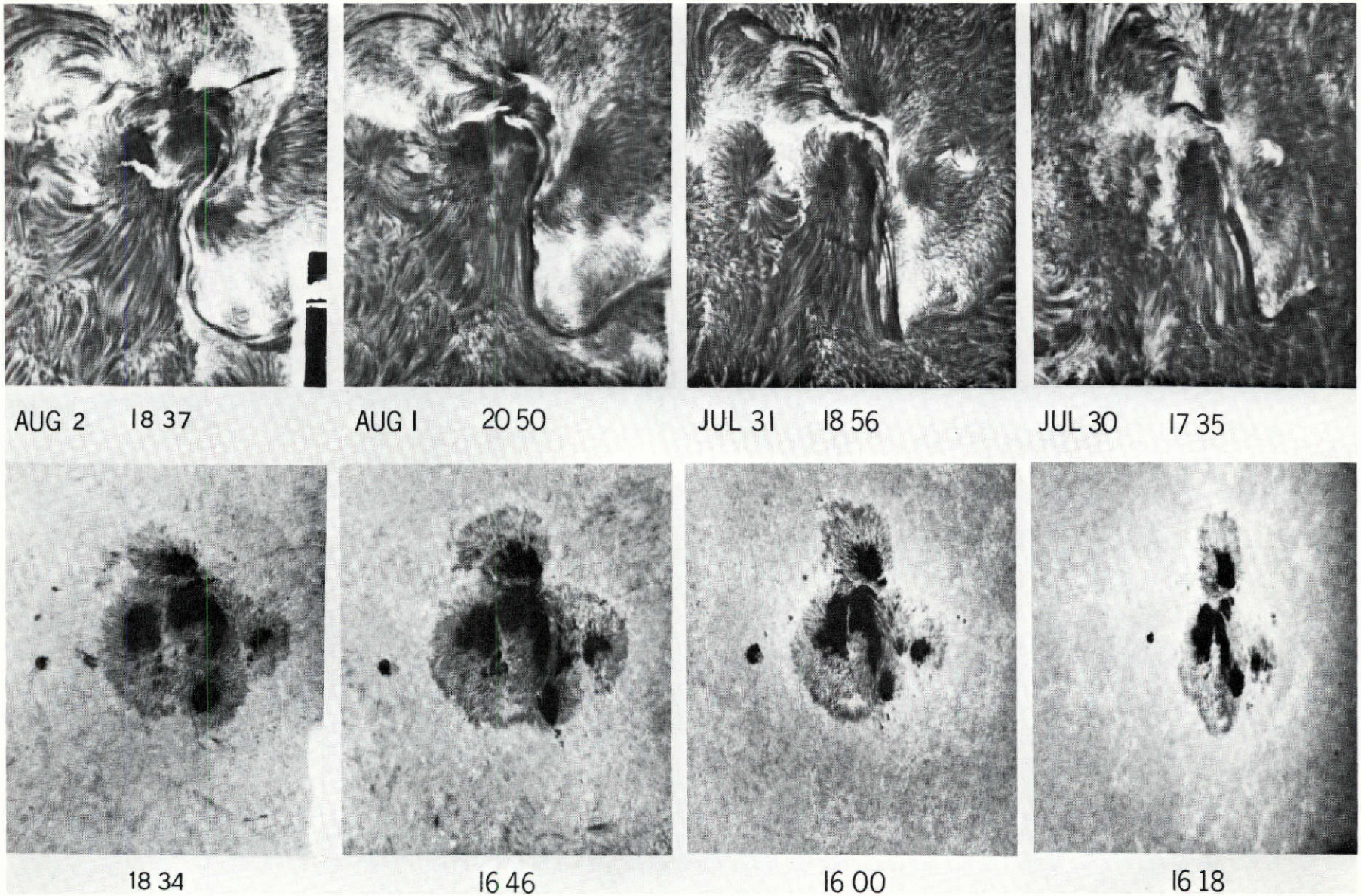

Figure 3

Synoptic series 7/30 - 8/2, with Hα centerline, best for plages and filaments, above, and Hα - 1.0 Å, best for sunspots, below. Note the rapid growth of the lower spot, designated f_1, and the increase of twist in the neutral line between f_1 and p_3.

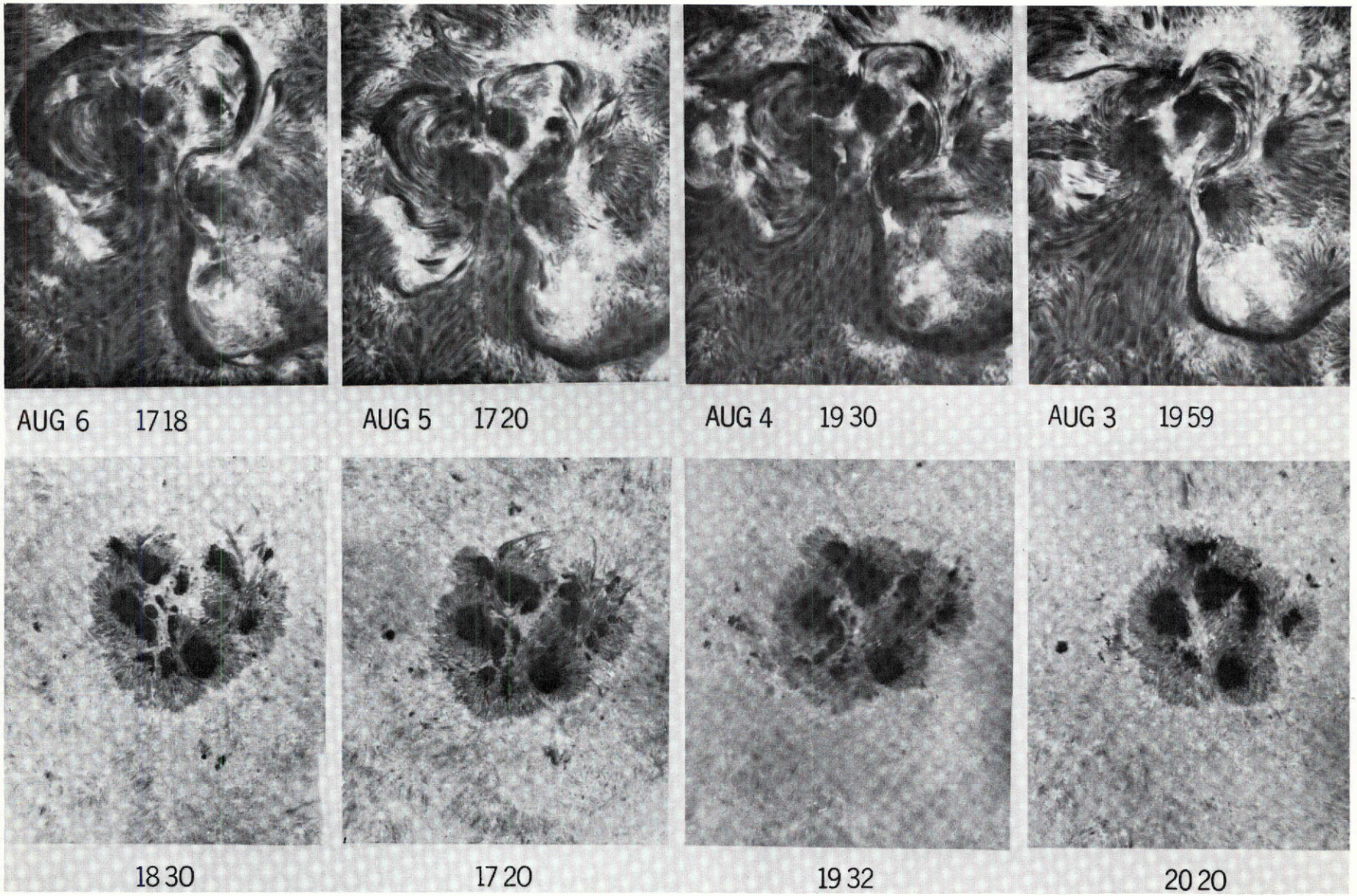

Figure 4

Further development, 8/3 - 8/6. Note the filament development and the E-W separation of the p spots. Note also the further increase of shear in the neutral line between f_1 and p_3. On 8/6 a complex double ring exists around f_2 in the main flare area.

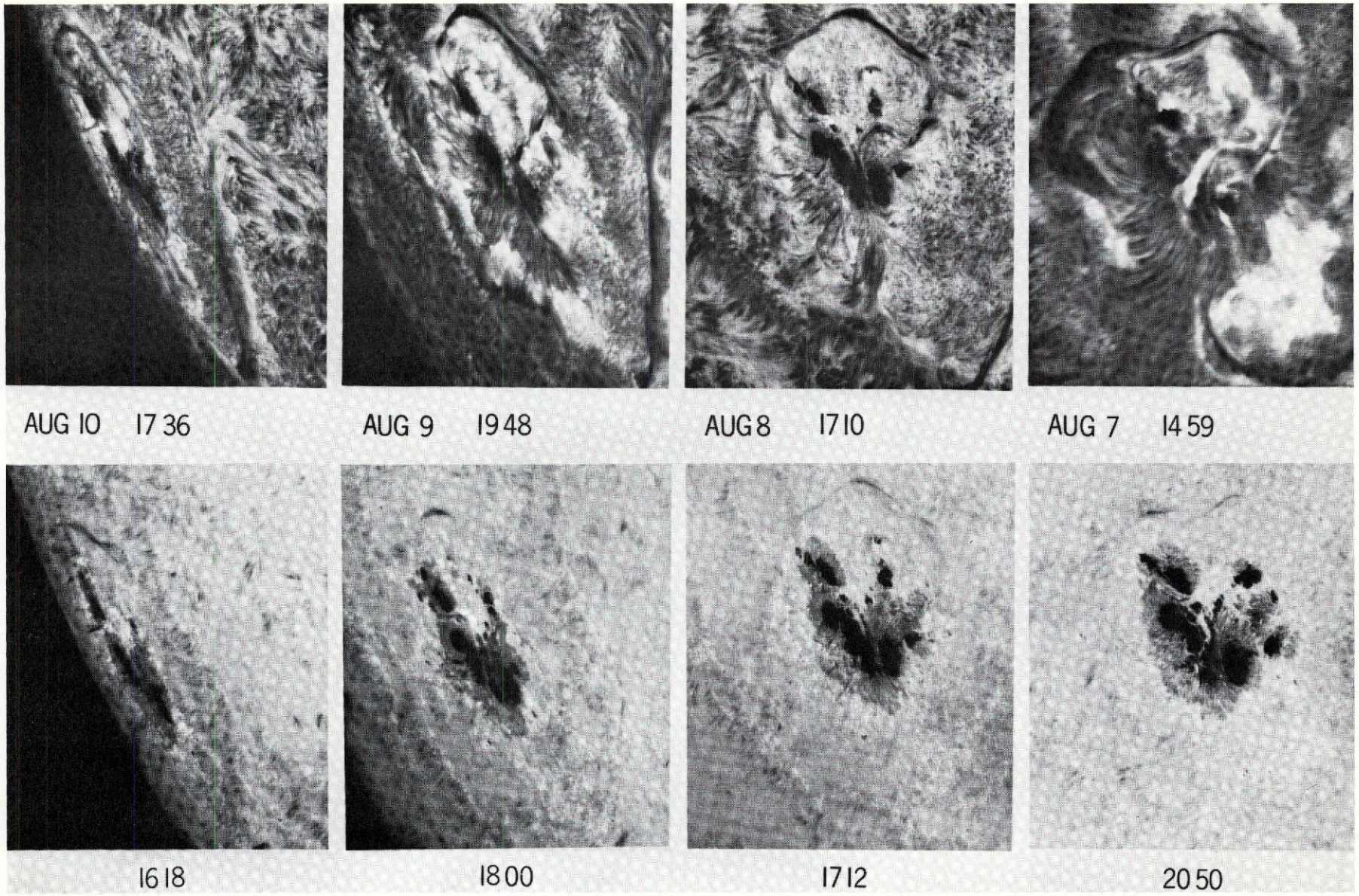

Figure 5

Development 8/7 - 8/11. The region simplified after the 8/7 flare. The 8/10 frames show how shallow is the vertical structure.

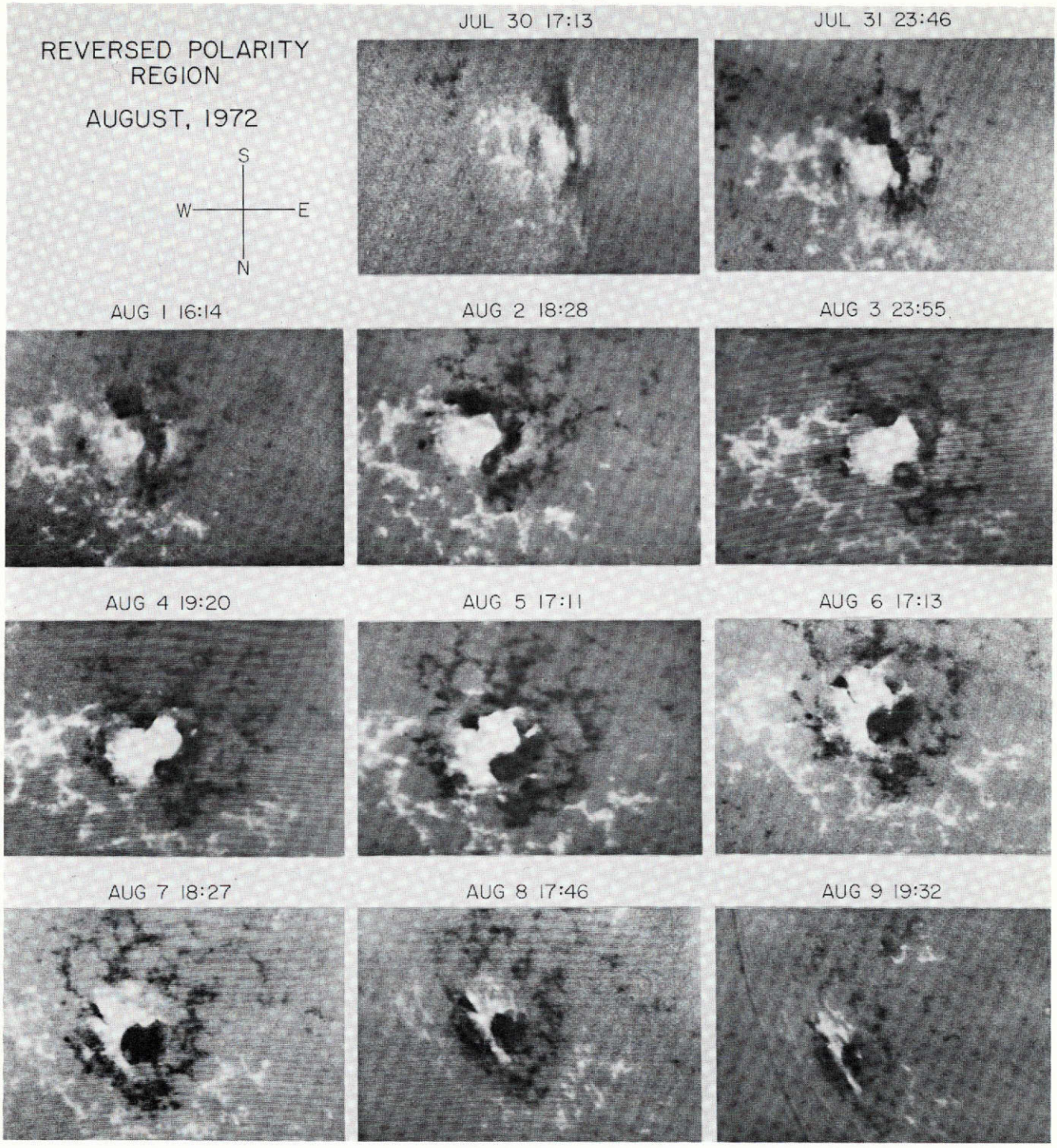

Figure 6

Videomagnetograms for 7/30 - 8/9. In this series white is preceding (p) polarity, dark following; the intensity of light or dark shading is proportional to the longitudinal field strength. The growth of spot f_1 is clearly seen as intense dark polarity below, and the eastward spread of p_3 is seen as the rightward spread of white polarity. Very rarely do such strong gradients appear.

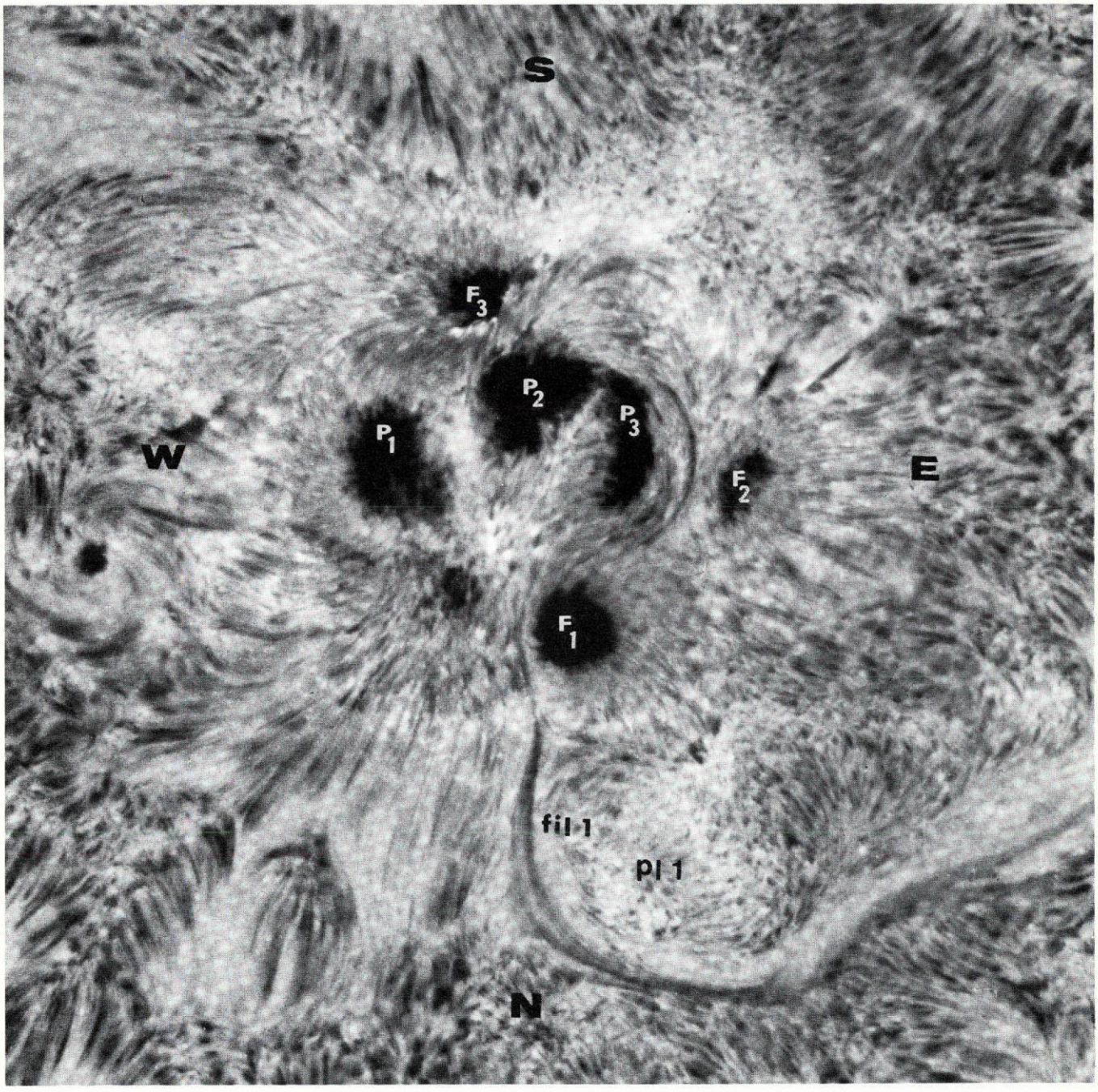

Figure 7

An enlarged frame 8/3, with various sunspots and areas marked to facilitate reference in the text. Note the strongly twisted penumbral structures.

way through the group.

The spot f_1, in particular, which seems to have produced most of the activity, was connected to p_2, whereas a much shorter, lower energy connection to the near part of p_3 was possible. The large *f* plage pl_1, enclosed by the filament *fil 1*, which did not form completely till August 1, was sharply bounded on the left (west) by the filament, with horizontal polarity only a few thousand km away. Note that the neutral line was almost N-S on August 1 and became sharply kinked afterwards.

The spot f_1 was indeed remarkable, and more so as it grew. It shows normal longitudinal spot polarity in the magnetogram, but the overlying Hα fibrils show transverse field a few thousand km above, so the field makes a sharp turn. Because the spot grew so rapidly it must be half of an emerging flux region (Zirin, 1971), but where is its sibling *p* polarity? The sibling appears to be the spot p_2. This spot and f_1 are seen to be connected by dark fibrils which are bright and active at both ends. Several flares (such as Figure 4, 8/3) are bright at both points. But these fibrils, in contrast to the normal arched filament systems, are strongly twisted and not prominent in pictures off the center of Hα. The spots separated as in normal emerging flux, but opposite the normal direction--the *p* polarity moved east and the *f* polarity west.

A particular feature of this group was the sharp twisting of penumbral fibrils seen in white light pictures and in Hα

off-band pictures as well, to run parallel to the neutral line. Such a twisting means that the sunspot field, which normally falls off like $1/r^2$, as the penumbral fibrils radiate outward, is confined to a narrow corridor of sheared fibrils, and the horizontal field in this corridor may reach spot values (i.e. 2000 gauss or more). This feature of sheared penumbras is common in regions giving big flares (e.g. August 28, 1966, Zirin and Lackner, 1969).

On August 1 there were continual bright flashes along the neutral line, and by the end of the day, two areas at opposite ends of the neutral line, near p_2 and f_1, were growing steadily brighter. The spot f_1 was completely covered by horizontal fibril structure. These fibrils go south from f_1, and, crossing above f_1 are fibrils going N from p_3. Since the fibrils must lie along the field lines, there were at least two polarity reversals above f_1, which of course must have longitudinal polarity. Fibril crossings of this type are common before flares.

IV. FLARES OF AUGUST 2

Major activity began in the region on August 2 with a remarkable series of complex flares. The first great flare was reported at 03:16 U.T. by Teheran; the later phases or perhaps a resurgence (two flares were reported but only one radio burst) are visible on our Tel Aviv photograph of 05:47 U.T. (Figure 8). This shows a large flare with bright strands covering all the spots, the brightest portion being over f_2. It differed from the later flares in that the *p* emission was confined to the spots and an area directly west. The long, dark filament following the group had disappeared, blown away by the flare. It reformed in bits and pieces, was blown away again by the later flares, and was whole again on August 3. By contrast, the great flares of August 4 and 7 only made it wave about. Whether or not the flare was associated with changes in the magnetic field structure, there were definite changes on the 1st and 2nd; the spot f_1 grew, and the spots f_2 and f_3 shrank, so that at August 2, 16:00, f_1 was bigger than the other two (eventually f_1 became the largest spot in the group). Spot f_1 also pushed ahead (W) relative to the other spots, as can be readily seen from the illustration (Figures 3 and 4); by August 2nd, the neutral line marked by the filament was directly beneath (N) of the *p* spots. A remarkable change also occurred in the fibril structure preceding the spot f_3. On the 31st, this was directly above (S) of p_1 and very close to

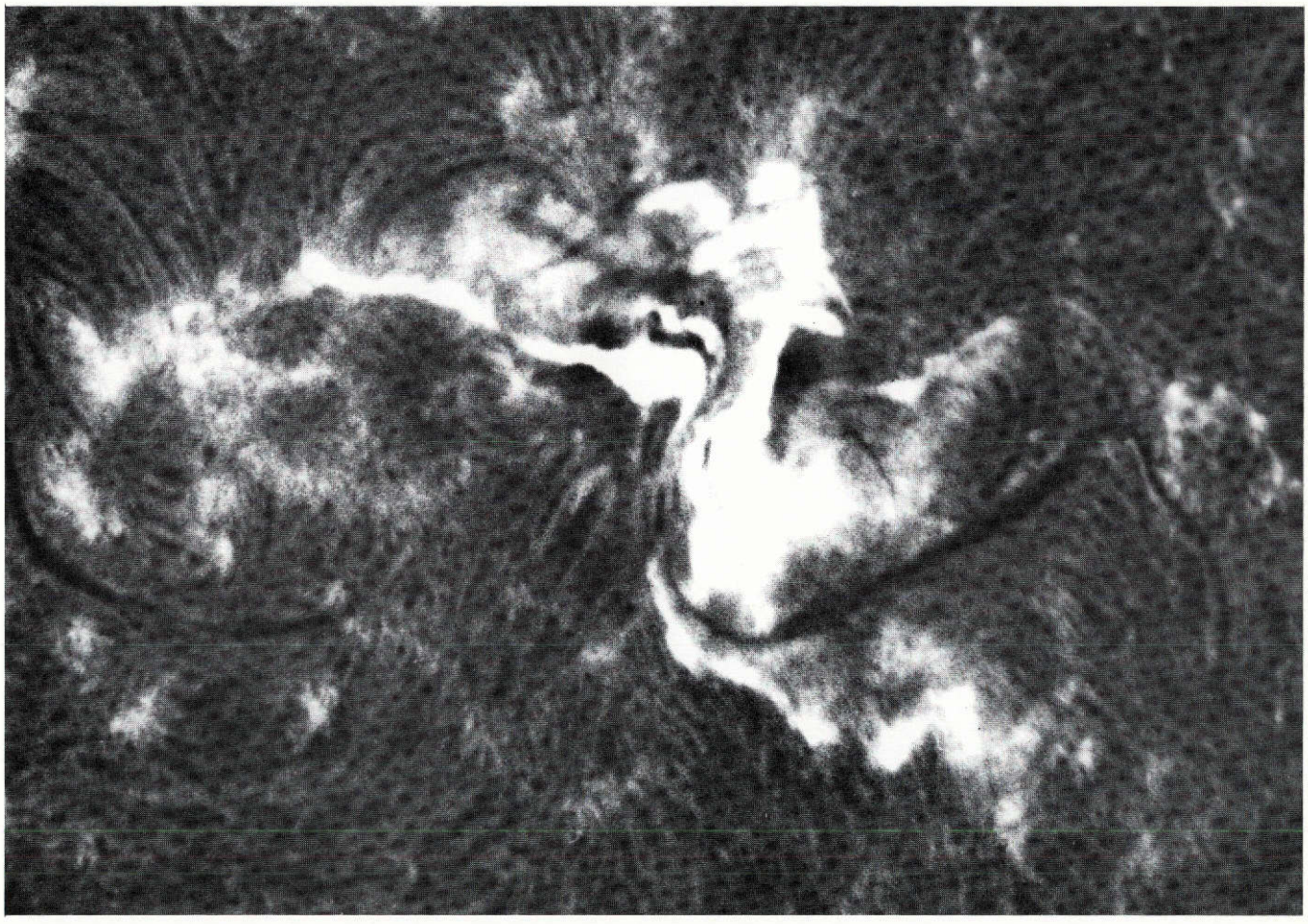

Figure 8

First flare, August 2, photographed at Tel Aviv, dawn, by Shlomo Hoory in Hα centerline. This photo at 05:43:38, more than two hours after the flare began, shows that it was similar to the later great flare.

f_3, almost along the neutral line dividing p_1 and f_3; on the 2nd (after the first flare), the fibril on the neutral line had moved considerably ahead (W) of f_3 and a new fibril system connected f_3 to p_1, with f_3 rapidly decaying. We have noted before that a sheared neutral line can be replaced by shorter lines going directly across the neutral line to the nearest opposite polarity; this appears to occur in this case. The flux in f_3 can disappear by shortening and eventual subsidence below the surface of the flux loops. The energy released in this flare would presumably be the difference between the elongated sheared lines and the shorter field lines of the final configuration. This difference was actually observed during later flares; for example, in the flare 18:38, August 2, a rapid break-up of the filament into shorter fibrils occurred at 18:37 U.T., one minute before the brightening started (Figure 9). For the flares of August 4 and August 7, we could see the bright flare loops cross the neutral line with increasing tilts, late in the flash phases (Figures 18 and 19). If there is a further contraction involved in the subsidence of field lines below the surface, this energy too is available for the flare. In succeeding days f_3 moved considerably closer to p_1 and thus lowered the total energy.

On August 2, Big Bear observations were made in Hα centerline and 3835 Å. After a small flare along the neutral line at 16:01, a brilliant impulsive flare began at 18:38. Its development is shown in dark prints in Figure 9 and in normal prints in Figures 11a and 11b. The flare occurred along the

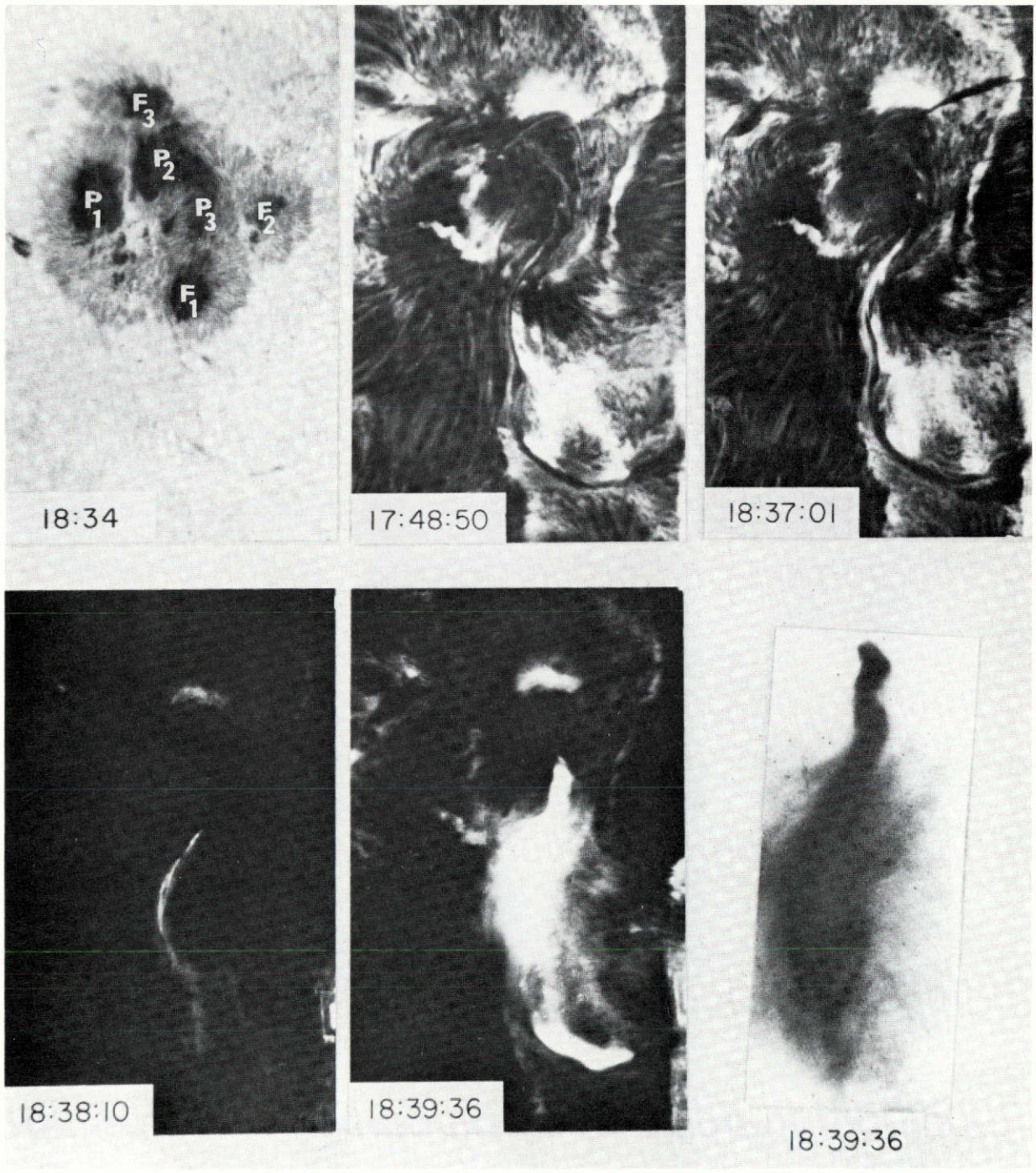

Figure 9

A series of prints made to show varied aspects of the 18:38 flare (18:34) Hα + 1 Å, showing spot structure, with spots marked. Note that all the spots lie in one penumbra, and the umbrae and penumbrae of f_1 and p_3 are twisted to follow the horizontal lines of force, rather than the normally radial structure.

- (17:48:50) - Hα before the flare. Note that the filament is sharp.
- (18:37:01) - The filament begins to break up into shorter fibrils.
- (18:38:10) - Dark print of flare beginning.
- (18:39:36) - Brilliant halo around the flare, probably Hα scattered by surrounding chromosphere.
- (18:39:36) - Light negative print, heavily dodged to show the structure of the flare kernel.

neutral line between f_1 and p_3 following a break-up of fibrils on the neutral line (Figure 9, 18:37) and spread rapidly along that line; there was a fast increase at 18:39:02 and another rise to a peak at 18:39:36; these coincide with an early hard x-ray peak at 18:39:00-10 and a main peak at 18:39:30-40. The dark prints, Figures 9d and 9e, and the negative print, Figure 9f, show the structure of the kernel. (The kernel consists of chains of bright points along the neutral line with an area of $3.8 \times 10^{17} cm^2$ and a diffuse halo with an area of $2.1 \times 10^{18} cm^2$.) This was the most brilliant flare we have yet seen in Hα, although its limited area kept the total fluxes down. This was not a classic two-ribbon flare; however, in the late phase (18:45) two emission strands were seen with a large shear, confined in the inner edges of f_1 and p_3. The two ribbons may have expanded, but the wall of the strong fields in f_1 and p_3 would have prohibited further expansion across the umbras. At 18:41 fast ejection of material was observed along the neutral line to the north of f_1.

Figure 10 shows how a sequence of brilliant fast flashes along the neutral line occurred in 3835. They occurred precisely at the W edge of umbra f_1 and the E edge of umbra p_3, showing how close to the edge of the umbrae the field became horizontal; flashes above either umbra or penumbra would probably have been visible, but were not seen. The average lifetime of the points was 5 to 10 sec (frame rate was 5 sec) and their individual size can be seen to be less than 1 arc sec, although some appeared in groups and had larger area (for

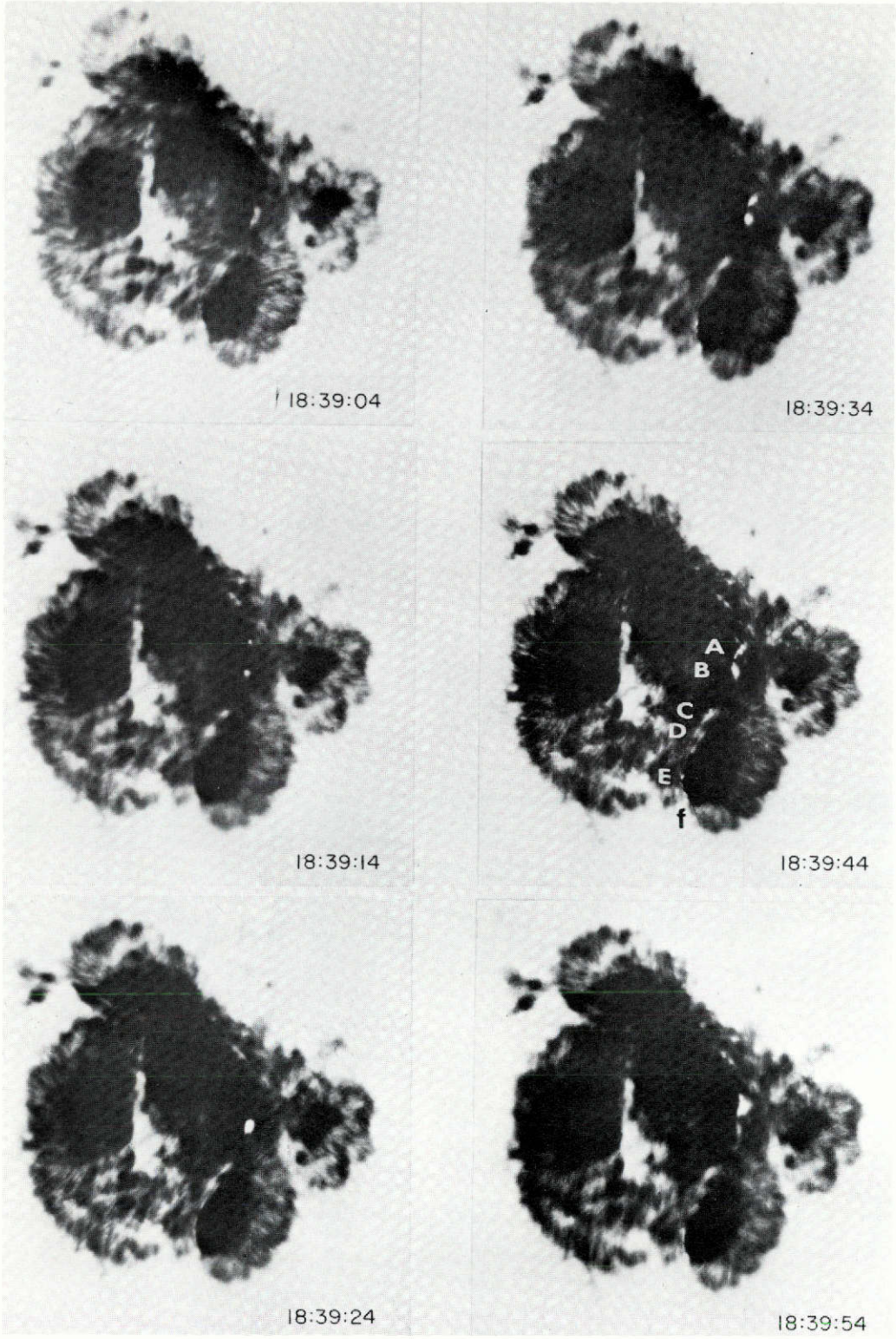

Figure 10

Dark prints showing the flashes in 15 Å band centered at 3835 Å. The point D (18:39:44) at the two bright strands on the left edge of the spot coincide with the Hα maximum. All flashes occur precisely at the edge of the umbras, where the field lines turn and intersect the surface. These pictures are taken with a corrector designed by the late Professor I.S. Bowen to remove the aberration of the singlet lens; unfortunately it was not properly adjusted and there is some astigmatism.

example Figure 10 (a), (b) and (c) at 18:39:44). The double bright strands (d) in Figure 10 mark the Hα center, and presumably corresponds to the usual *p* and *f* polarity strands, but are much closer. The strands (d) and point (b) rose with the first x-ray pulse, then broke up into faint points; a new bright point appeared at 18:39:24, as the flux rose. It faded in 10 seconds, and a row of points flashed into view at the x-ray maximum, 18:39:34. The points appeared in symmetric pairs such as points (a) and (e); the lower points are less visible. As time passed, more points appeared to the north edge of f_1. By 18:40:00, no more flashes were seen except for the lingering of point (f), which was under a long-lived Hα flare knot.

We interpret the 3835 flashes as occurring at the intersection of flux loops with the surface; the emission must be due to the heating of the lower atmosphere by energetic electrons as they are accelerated in individual flux tubes and give up their energy at the surface. Thermal conduction from the flare above as an alternative source of heating would not be able to explain the fast time variation and limited extent of the flashes; the collision frequency at these densities is sufficient to produce conductivity across the field line which would rapidly homogenize the temperature in the source region, making difficult selective and time-dependent heating of the lower atmosphere, as well as spreading the emission area. Detailed discussions of the 3835 flashes related to the x-ray and radio bursts will be given in the next chapter.

The activity of August 2 was not yet over; more flares

were to come. Although the filament *fil 1* was disrupted, it reformed and straightened again; bright areas resulting from the flare remained, particularly of the *f* edge of *fil 1*. At 19:57 the area below spot f_1 brightened slowly, then more rapidly after 20:01 (Figure 11c). A weak brightening in 3835 appeared at the most intense portion of the Hα flare. This flare reached maximum around 20:05 and remained stable; it produced a modest hard x-ray burst, but little radio emission; at 20:20 a new increase in area and brightness began on both sides of *fil 1* and at 20:30 yet another wave of brightening spread south from *fil 1*; this was matched by a bright region (Figure 12) in 3835 (twice the photospheric intensity) just at the edge of the advancing bright Hα front. At the same time the entire *p* side of *fil 1* brightened as well. The 3835 emission in this flare was not impulsive at all, lasting more than 15 minutes, although the lifetime at any point on the surface was only a few minutes. Again it appears to mark the footpoints of flux loops containing the energetic material (this time thermal conduction can be the heat source). The hard x-ray flux increased again and a large 6600 sfu, 8800 MHz burst occurred. The Hα front spread steadily on to a maximum at 20:50 (Figure 11d); the 3835 emission moved south with a constant velocity of 12 km/sec and changed its direction to northeast when it hit the edge of penumbra f_1 as if it was reflected by the spot field. The 3835 emission could be followed till 21:05, but by now the Hα emission near the filament was dying out and the whole flare faded, accompanied by fine

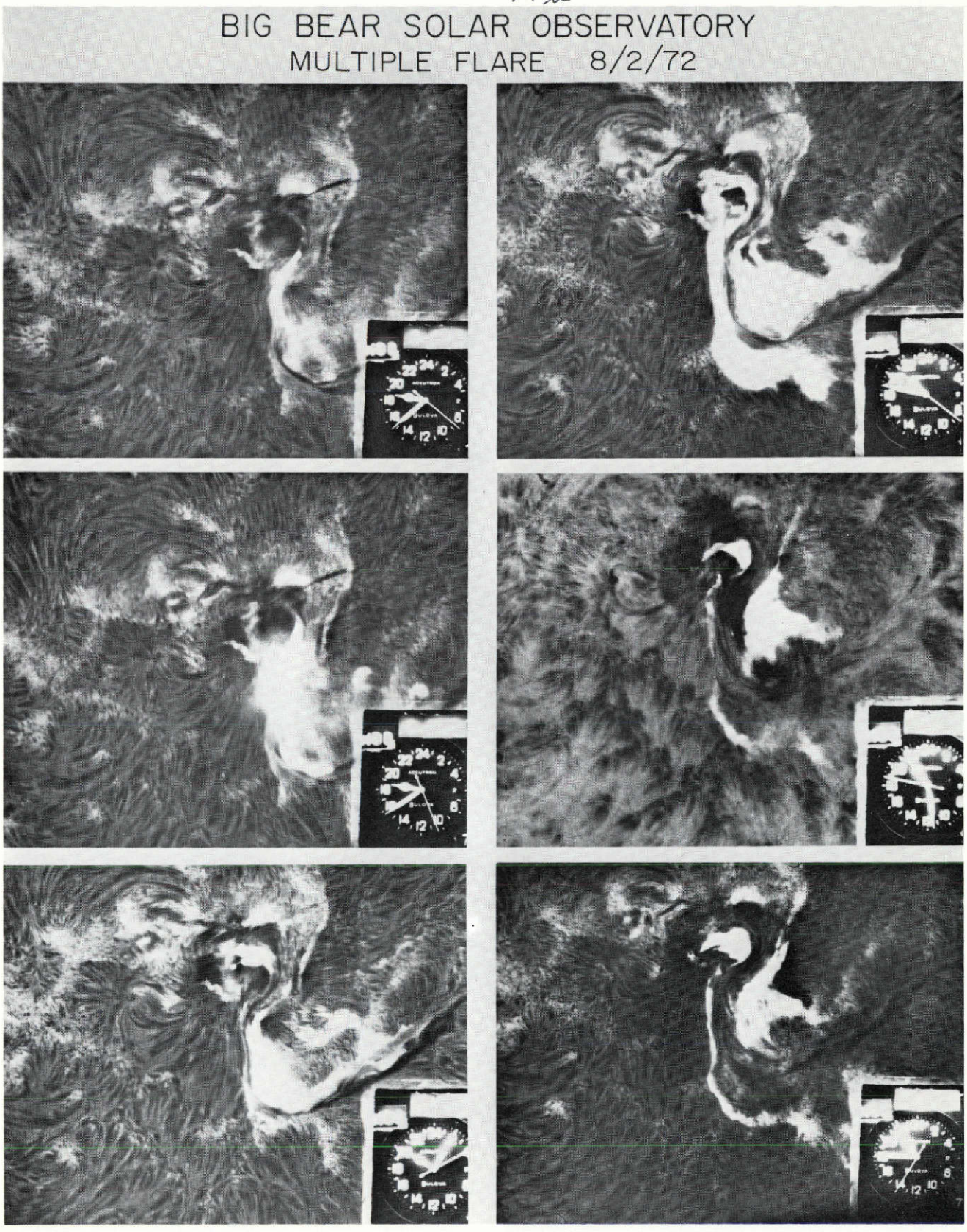

Figure 11

An Hα centerline sequence of the flares after 18:38. The fifth frame (21:28) shows an Hα + 0.5 Å picture which reveals the loops raining down after the flare; the last frame (21:45) shows the peak of the radio burst; note that the emission has shifted to an entirely different location from the fourth frame (20:47) and both f_1 and p_2 - p_3 are covered by emission.

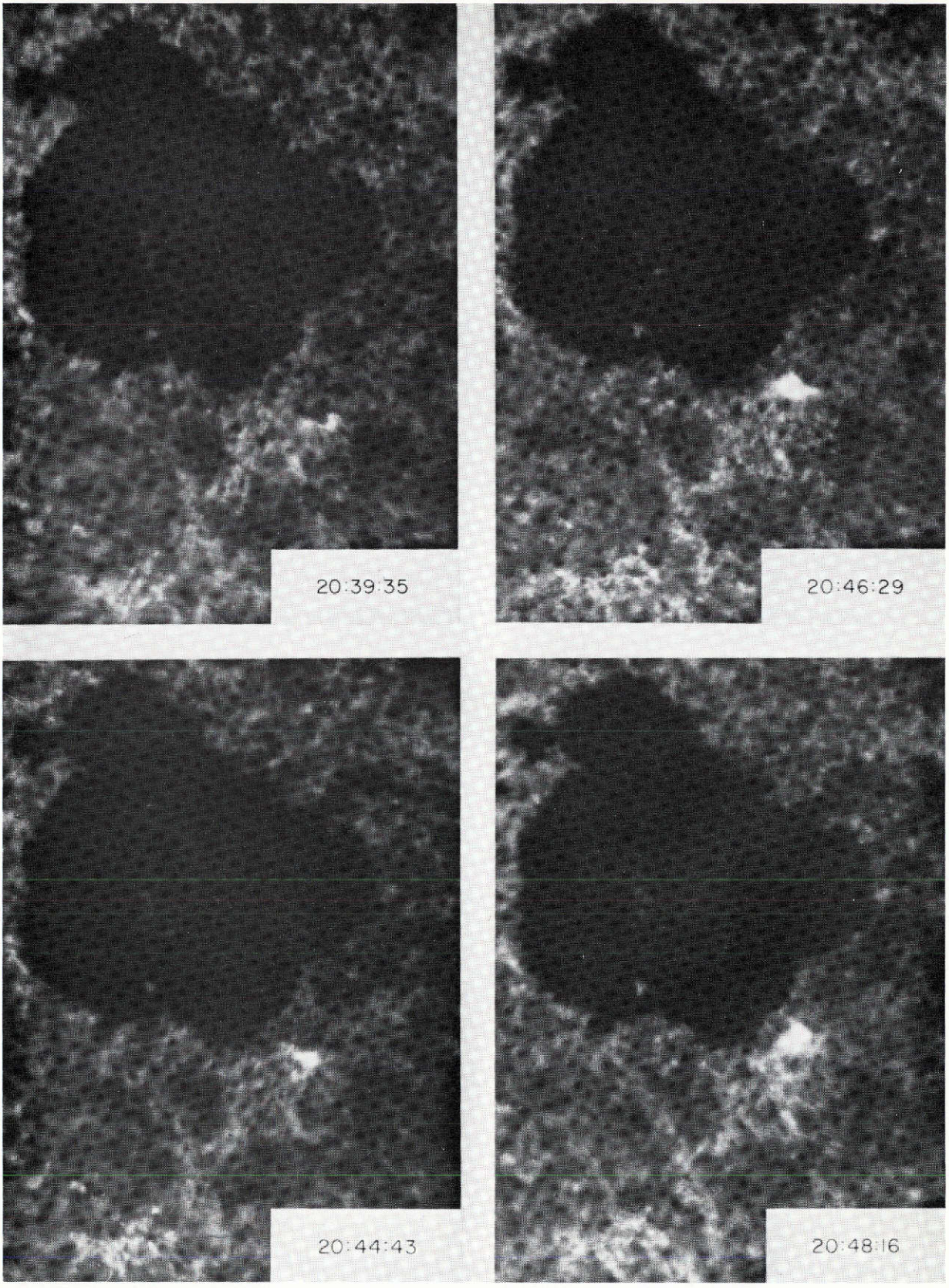

Figure 12

Dark prints showing the drift of bright points in the 3835 bands in the 20:35 flare of August 2. The bright points coincide with the Hα bright front (the fourth picture of Figure 11) and move toward spot f_2 with a velocity of 12 km/sec.

dark loops. But the last bright parts of this flare, spreading over p_2 and f_1 (Figure 11e, f), produced at 21:40 the greatest peaks of radio and x-ray flux. Weak 3835 emission appeared at this time over the penumbra of p_2. Note that this is different from the decay of other flares, which leave two widely separated strands on the flare perimeter; the emission actually shifted to a different place, and was strong in off-band (Figure 11e), indicating broad Hα profile, and showed 3835 emission. So there was a real flare resurgence, particularly over the main umbra. The UCSD x-ray data shows a small resurgence of x-ray emission above 10 KeV but less than the peak of 20:50. So there were no more harder electrons, just a stronger magnetic field.

The varied aspects of the August 2 flares present an excellent opportunity to compare different flares in the same region. The comparison between the impulsive 18:38 flare--small, violent, short-lived--and the large, long-lived, slowly-rising flares at 03:10 and 20:00 is most instructive. The first was physically low in the atmosphere, confined to the neutral line in a small region, and by far the most brilliant and concentrated. It also produced the short-lived, intense hard x-ray burst with a spectrum proportional to $\nu^{-3.5}$. The 3835 observations show the impulsive nature very well. Radio emission was low below 2700 MHz, indicating a low source height (because of plasma cut-off or other high density absorption).The 03:10 and 20:00 flares were by contrast complex and slow, with longer rise times both for Hα and

energetic electrons, and radio emission appeared at low frequencies, showing that the events reached high in the atmosphere. Since radio flux and x-rays are proportional to the total number of electrons, we can see how the large volume involved produced the huge radio bursts. However, these large events were less impulsive and had a steeper electron spectrum, so high frequency radio emission was less; for example, at 35 GHz the 21:40 peak is only slightly higher than the 18:39 peak, although it is 20 times higher at 8.8 GHz. We may conclude that slow events may accelerate particles quite well, but that impulsive, low-lying flares produce the hardest spectra. Finally we have the peculiar effect of the greatest radio burst occurring late in the event without an accompanying large change in the optical flare; apparently once the hard electrons are produced, phenomena over the greatest spots can produce great fluxes of radio emission (because the emission is proportional to B).

Huancayo polarization data published by Lincoln and Leighton (1972) show a sharp variation from left to right hand circular polarization at 9400 MHz, then back to left, in the 18:38 flare, whereas the 21:00 flare shows only right hand polarization. This corresponds to the fact that the later flare occurred primarily in the following (= N polarity = rhc polarization) part of the group (see Figure 11e, how *f* area is large compared to *p* area), while the impulsive flare was on the neutral line where changes in the polarity balance could easily occur. The August 7 flare was also found by

Huancayo to show such a L-R-L shift in the impulsive phase. In both cases, the largest sunspot in the flare region was f_1, so that following polarity would dominate the radio propagation.

V. THE 3835 FLASHES AND IMPULSIVE BURSTS OF X-RAYS AND MICROWAVES

The 3835 flashes in the 18:38 flare of August 2 occurred simultaneous with the impulsive hard x-rays and radio bursts. Since good data were obtained in UCSD x-ray experiments and at Sagamore Hill for microwave bursts, it would be useful to compare these three wavelengths for better understanding of electron accelerations in the impulsive phase.

Figure 13 shows comparison of the light curves of several 3835 flashes with x-rays and radio bursts. Each light curve was made by measuring the brightness of a 3 arc sec^2 area which showed several resolved and/or unresolved flashes in the whole lifetime (1 minute) of the flashes with a mean lifetime of an individual flash less than 10 seconds. (For example, in Figure 10 point (a), the topmost at 18:39:44, is made up of at least 5 points.) One can see that the intensity of the optical flashes peaked around the same time as the x-ray and radio bursts and that the light curves are more similar to the x-ray bursts above 50 KeV than to the 14-20 KeV x-rays or radio bursts at 5000 MHz. In addition, Figure 10 shows that the first flashes appear at 18:39:04 simultaneous with the first x-ray spike, and the most flashes were seen at the peak around 18:39:40. The x-ray spectrum was proportional to $\nu^{-3.4}$ at the peak and softening of the spectrum began from 18:40:10 (Datlowe, private communication).

The observed intensity of the 3835 flashes can be explained

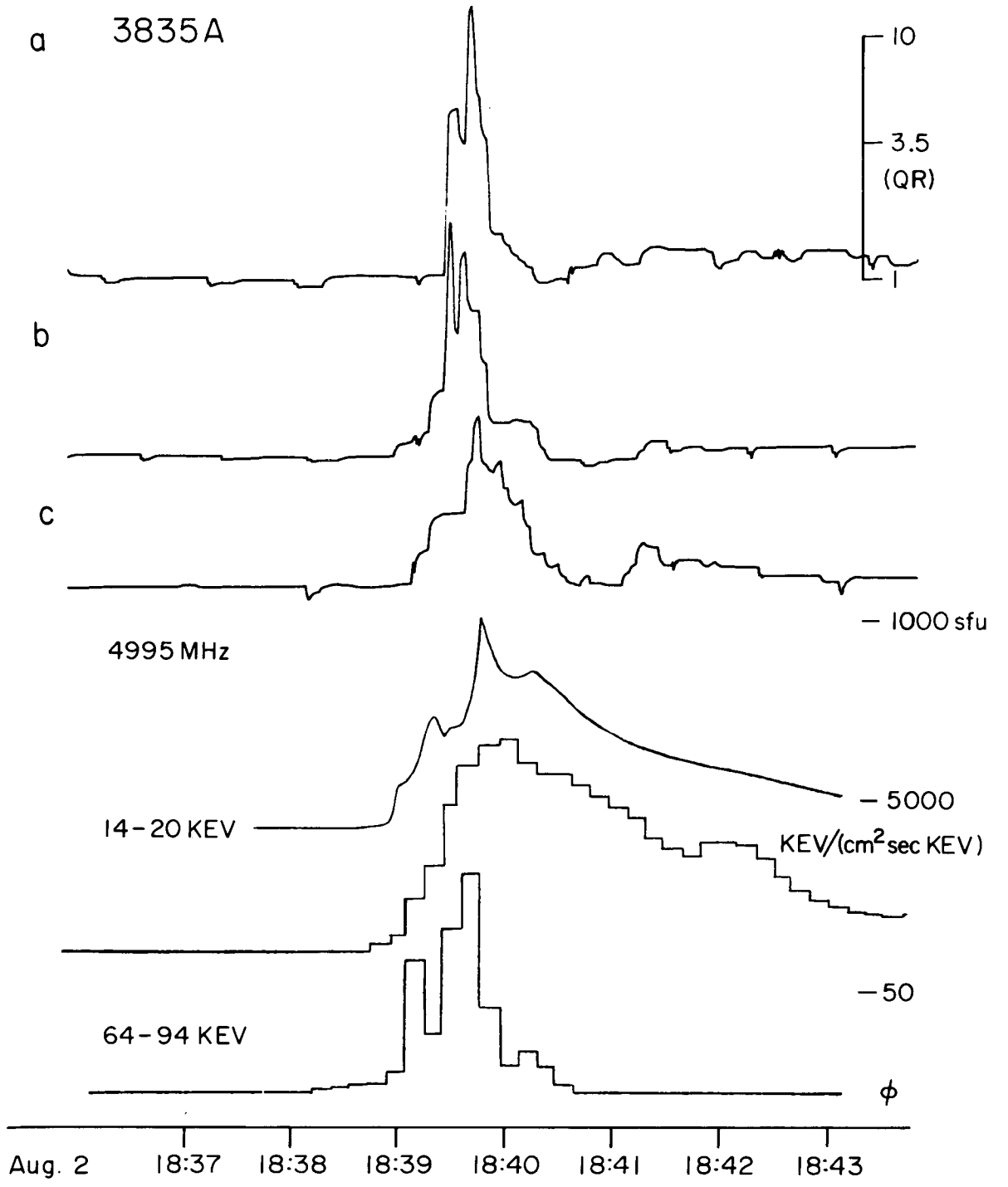

Figure 13

Light curves of the 3835 flashes measured at three positions (see Figure 10 for identifications of positions). The lower three curves show a microwave burst (Sagamore Hill) and two channels of hard x-rays (UCSD). Note that the time histories of the 3835 flashes are most similar to the 64-94 KeV burst.

by Balmer line (H9) emission centered at 3835 Å. When we look at spectra taken in another large 2B flare, November 18, 1970, observed by Tanaka (unpublished) at Okayama, we find wide and large emission of H9, which has 4 equivalent Å of the mean intensity level of 3835 region (20% of the true continuum). We require, in this intense flash, emission of H9 greater by a factor of two than the above flare; if we equate the observed flux at the peak of the flash (equal to the intensity of 3835 Å in quiet region) to $n_9 A_{92} h\nu H/4\pi$ (H: thickness of the emitting layer; A_{92}: rate of spontaneous emission; n_9: number density of level 9) we get $n_9 H \sim 1.7 \times 10^{14} cm^{-2}$. Assuming the Saha-Boltzman distribution with a temperature of $10^4 K$, we have $n_e n_p H \sim 4.2 \times 10^{33} cm^{-5}$ at the peak (n_e, n_p are electron and ion number density respectively). The total flux emitted by the flashes may be estimated by adding line emissions, free-bound and free-free continuum emissions radiated from this $n_e n_p H$. With a mean area of the flashes $6 \times 10^{16} cm^2$ (= 10 flashes) we have 2.6×10^{27} ergs/sec at the peak. Note that half of this energy flux is radiated in Hα. Actually in dark prints of Hα, we could see Hα brightening simultaneously with the 3835 flashes, but they remained bright after the latter disappeared because of the large opacity of Hα; precipitation of low energy electrons below 20 KeV, which existed till late as Figure 11 shows, or thermal conduction produced continued heating of the upper layer emitting Hα.

It can be shown from the x-ray flux that electrons above 45 KeV in the thin foil model and above 60 KeV in the thick

foil model have the same total energy as the optical flux estimated above. 50 KeV electrons can penetrate the column density $n_pH \sim 10^{20.4}$ as the theory of Coulomb collision shows (Schatzman, 1965; Shmeleva and Syrovatskii, 1972; Brown, 1972). Also from the observed production rate of 50 KeV electrons in the thick foil model (= $1.0 \times 10^{35} sec^{-1}$) it turns out that these electrons penetrating the chromosphere can ionize $7 \times 10^{20} atoms/cm^2$ -sec by making an ion pair every 33 KeV (Fermi, 1949; Hudson, 1972). Therefore we can explain reasonably the heating and ionization of the layer responsible for the 3835 flashes ($n_e n_p H \sim 4.2 \times 10^{33}$) by the dumping of the electrons above 50 KeV. We have $n_e \sim 10^{13.2} cm^{-3}$ and $H \sim 10^{7.2} cm$ for the emitting layer. Similarity of time profiles between the 3835 flashes and x-ray bursts above 50 KeV (Figure 13) would support this explanation. Because of confusion with the other flares we do not know if there was any proton production involved in this fast event, but the fact that γ-rays were not detected gives an upper limit of proton flux less than $3 \times 10^{26} ergs/sec$, below the energy flux of the optical flashes.

Optical evidence of electron precipitation seen in the 3835 flashes would give a more realistic image of acceleration; impulsive acceleration of electrons occurs in each individual flux loop with a time constant less than 10 sec and the place of acceleration moves around with the same time scale. Since the flux loops have small cross sections at their ends (0.5", size of the flashes) and stretch flat on the surface as Hα fibrils structure shows, the acceleration must have taken place

at a low height ($h < 10^9$ cm) and in limited regions. Thick target emission of x-rays (Hudson, 1972) is realistic since most of the electron energy is dumped in a short time at the high density layer. Even if trapped electrons exist and emit x-rays by thin foil, the emission must be small compared to the observed flux, which could be emitted in denser layers by electrons needed to explain the optical flashes.

Radio spectra observed by Castelli (Figure 14) show an increase of flux from 15 GHz to 35 GHz with a dip around 15 GHz. In coincidence with the end of the 3835 flashes and the x-ray flux in the hardest channels the flux at 35 GHz decreased appreciably showing a single peak spectrum by 18:40:40. If the dip in the otherwise flat spectrum is not an observational effect, it might be explained by free-free absorption due to hot ambient plasma, which has been proposed by Zirin et. al. (1971) and by Ramaty and Petrosian (1972) to explain flat type spectrum. In order to realize a dip in the spectrum, it turns out that there must be an optically thick plasma for free-free absorption at the frequency at least 40 GHz. Since hot plasma emitting soft x-rays is transparent for free-free absorption down to 4 GHz as the observed emission measure and temperature show, lower temperature material such as produced the XUV flash must be invoked for the absorption in this model. The double-peaked spectra may also be interpreted as originating from two sources; one at the top of the flux loops, where acceleration takes place with lower magnetic field and plasma density and giving a peak at 5000 MHz, and the other is located

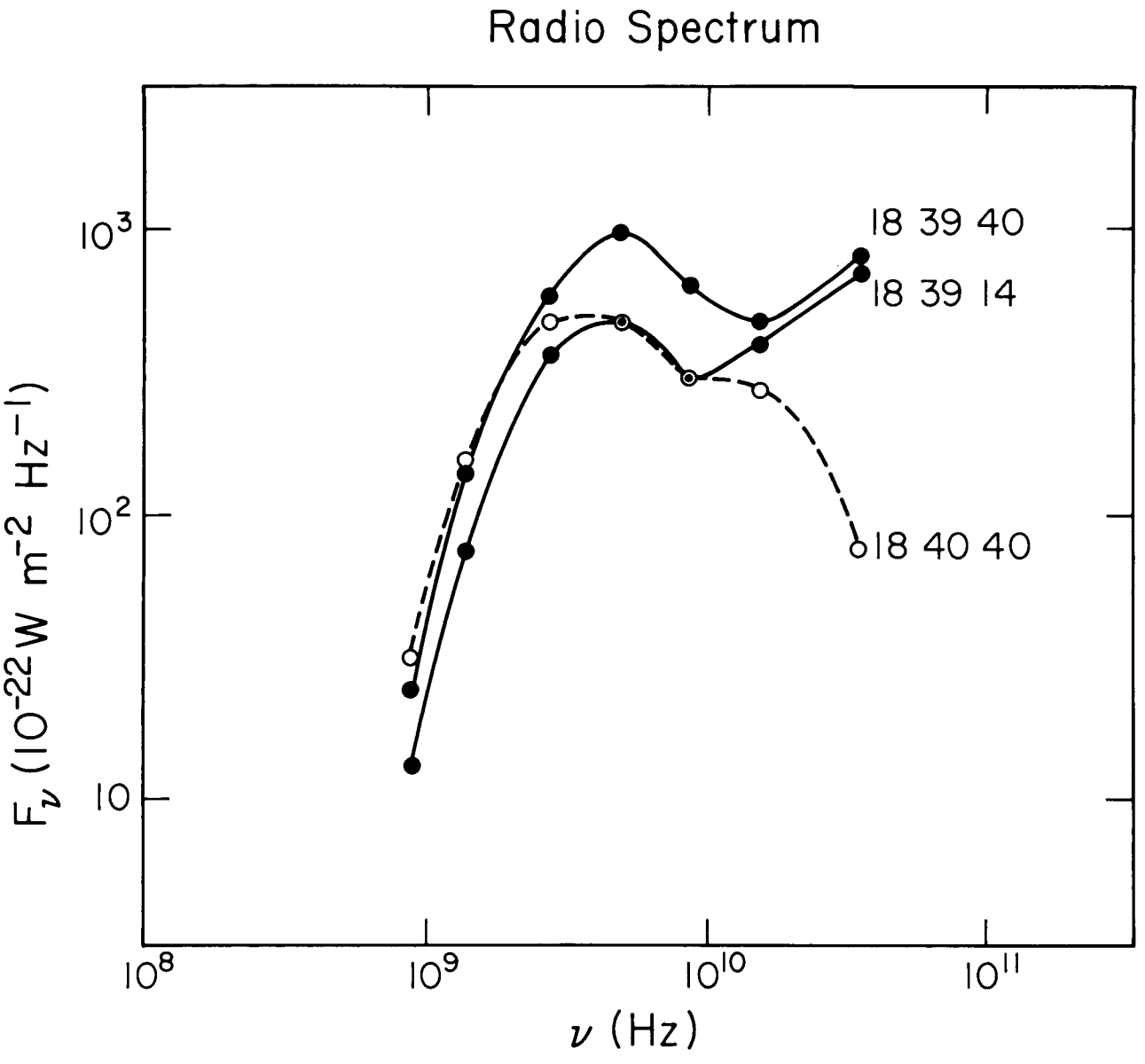

Figure 14

Microwave spectrum for the 18:38 flare of August 2 obtained by Castelli. Note the rapid decrease of the flux at 35 GHz after 18:40, which was in coincidence with the end of the 3835 flashes.

at a lower height near the mirror points with a stronger magnetic field and a peak beyond 35 GHz; the flux around 15 GHz may have been depressed due to cut off by plasma frequency or Razin effect or free-free absorption of low-temperature material. These two sources may well correspond to Hα bright points and diffuse halo respectively (Figure 9).

For these two models we may estimate the number of electrons needed to explain the radio fluxes and compare these with x-ray observations. In the case of a homogeneous source model with a free-free absorption, we have a total number of electrons above 100 KeV (denoted as N_{100}) equal to 10^{34} - 10^{35} by fitting the observed spectra to those calculated by Ramaty and Petrosian (1972). This number is not inconsistent with $n_i N_{100} \sim 10^{45.6} cm^{-3}$ derived from the x-rays by assuming thin foil although the thin foil model is not realistic for explaining the 3835 flashes. In the thick foil case we have $\frac{dN_{100}}{dt} \sim 1.6 \times 10^{33}$ sec^{-1}; so accumulation of injected electrons for 10 seconds or more is necessary. This does not agree with the thick foil picture. On the other hand, when we consider a flux loop model in which acceleration takes place continuously for 10 seconds or less at the top, and electrons dump at the two ends of the loop emitting x-rays there by thick foil, the total number of electrons in the flux loop at any instant can be determined by the continuity equation along the flux loop: $v \frac{N_{100}}{L} = \frac{dN_{100}}{dt}$, where L is a length of flux loop. With $v \sim \frac{C}{2}$ and $L \sim 2 \times 10^9 cm$ (observed mean distance between pair flashes) as well as $\frac{dN_{100}}{dt}$ from the thick foil model we have $N_{100} \sim 2.1 \times 10^{32}$,

in agreement with $N_{100} \sim 10^{32}$ obtained for the 5000 MHz peak of two source models. To derive the latter number, optically thin gyrosynchrotron emission is assumed with the peak emission occurring at $3\nu_B$ (Takakura, 1967) since self-absorption would be negligible in a small cross section of a flux loop such as is considered here. ($N_{100} = 10^{32}$ together with B = 500 G and $A = 2 \times 10^{18} cm^2$ gives a self-absorption factor $\frac{N}{BA} \sim 10^{11}$, which agrees approximately with the calculated curve by Ramaty and Petrosian (1972) if we adopt the electron power equal to 4.5 obtained from the thick foil in this case.) For the higher frequency peak we get a similar value for a magnetic field larger than 1000 G although we don't know the exact frequency and flux of the peak. Thus we can explain the radio flux in this simple model of a flux loop consistently with thick foil x-ray emission and the 3835 flashes. It is to be noted that the electron distribution exponent γ ($N(E) \propto E^{-\gamma}$) derived from the high frequency slope of the radio spectrum at 18:40:40 (single peak) is equal to $\gamma = 4.7$, in agreement with $\gamma = 4.9$ derived from the hard x-ray spectrum assuming thick foil. In the thin foil model, on the other hand, we have $\gamma = 3.0$, inconsistent with the radio value.

VI. DEVELOPMENTS AUGUST 3 TO 4

After the great events of August 2, the region changed rapidly: the spot f_1 continued to grow and plow into the *p* region, p_2 and p_3 split apart and a small EFR appeared between p_1 and f_1, eventually producing some new *p* spots. The axis of p_2 - p_3 rotated rapidly as p_3 moved eastward, producing further shear along the neutral line. A series of small flares occurred during August 3, the largest being at 22:10, with arms around f_1 and area between p_2 and f_3, where f_3 was approaching ever closer to p_2.

When the sun rose at Tel Aviv on August 4, a great flare was beginning; observations began at 06:24, showing the flare rising to a peak area at 06:35. But the most rapid rise occurred between 06:24 and 06:27, coinciding with steep rise and peak in the radio burst. The Hα flux 1.0×10^{27} erg/sec (using August 7 line widths) was constant from 06:25 U.T. to 06:45 U.T. and decayed slowly. As on August 2, 21:45, the greatest peak in the radio emission came with brilliant emission covering the *f* spot. Figure 15 shows the peak of the flare photographed at Tel Aviv. It was a classic 2-strand flare, with most of the area in the *f* polarity, and it did not have the irregular growth of the August 2 and 7 flares, nor was it so impulsive as the much smaller event of 18:38 August 2, although a rise in radio flux of 26000 sfu in 3 minutes is certainly not sluggish. Thus its radio spectrum fell off somewhat above 8.8 GHz. The radio flux reported by

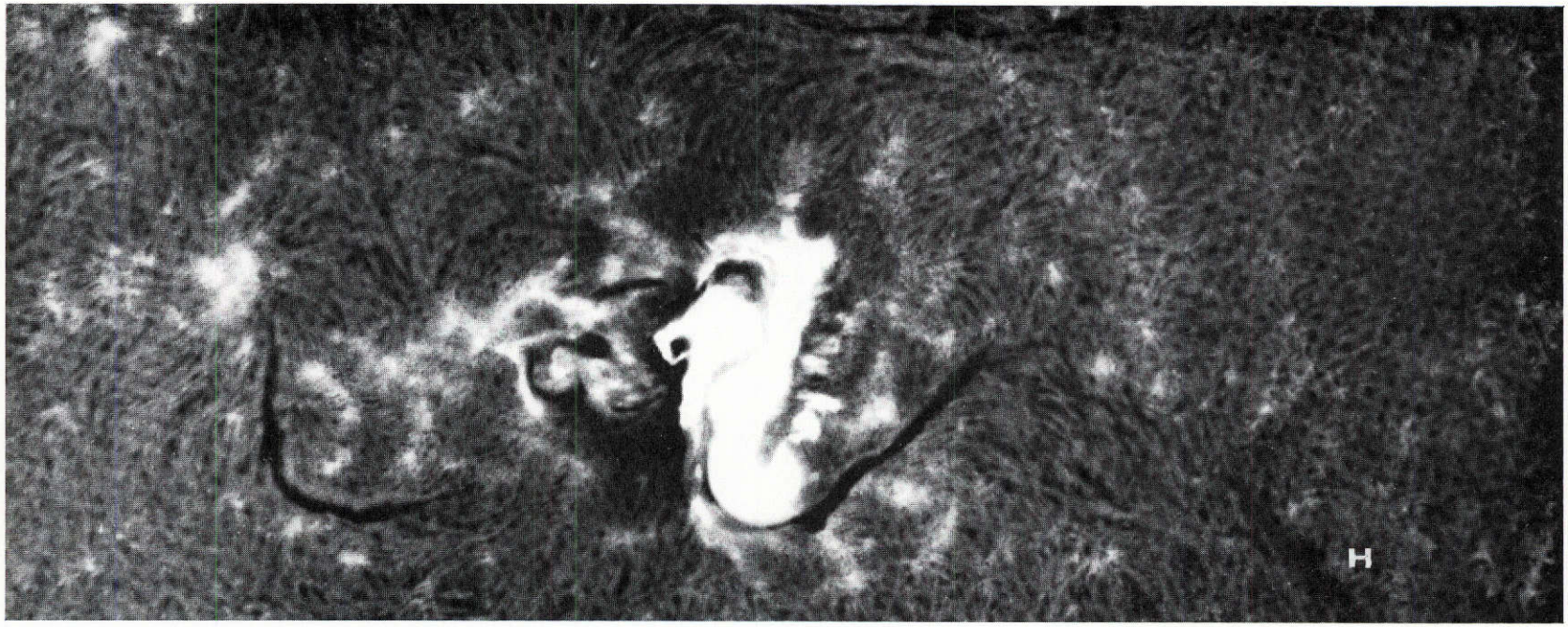

Figure 15

Maximum of the August 4 flare, 06:34:19, photographed at Tel Aviv. This is a classic two strand flare, leaving two faint thin rims at the extreme edges for many hours. The filament H was disturned by the flare.

Slough dropped off after the flare passed maximum. At 06:42, a group of bright loops passed across from the *p* to *f* side, filling the space between the two strands; these became dark 10 minutes later. Again, although the field lines on the surface run tightly parallel to the neutral line, the loops high above are perpendicular. We see the loops increase their tilts to the neutral line continuously with time (see curve in Figure 19 for this change). The bright strands faded and separated, leaving two thin strands at the farthest points from the neutral line, lasting many hours. This, and the slow decline of thermal x-ray emission (e-folding time equal to 150 minutes), shows how the coronal cloud produced by the flare cools from the surface outward, leaving only the outermost loops at the end. These loops presumably produce the Hα strands by thermal conduction at later phases.

No Moreton wave appears on the film; although the observations are in Hα centerline, a Moreton wave should be visible. However, a section 0.6 $R_\odot$ from the spot of the long filament stretching E of the spot (*fil 1*) disappeared at 06:26; and an emerging flux region 0.7 $R_\odot$ from the flare brightened about the same time. These distances imply a wave moving 1000 km/sec from a source at 06:18 (the earliest reasonable time, judging by radio data), but moving above the chromosphere so that it is seen only indirectly. More interesting, a bright wave or spray moved out from a point in the filament about 0.6 $R_\odot$ from the flare at 06:24, with a velocity of 250 km/sec. This wave, which moves irregularly N-S from the filament, looks like a

slow Moreton wave. If it was triggered by an invisible wave from the flare, we again get 1,000 km/sec for the velocity. This is the first case we know of of such a spray being produced by a wave. The filament waved about continually until 08:00.

Uchida (1972) has shown that the Moreton wave may be considered as an MHD wave which only touches the surface when it reaches a region where the Alfven velocity is low and a steep shock develops. It may be that the wave in question did not touch the surface, but was able to affect the chromospheric features it passed by perturbing the field structures. The apparent triggering of a slower wave from the prominence is obviously a more complicated problem, either involving energy stored in the prominence or refocusing of the wave energy.

VII. DEVELOPMENT AUGUST 4 TO 7

In the BBSO pictures for August 4, we can recognize several changes which may be connected with the August 4 flare. f_1 and f_2 had grown, and the spot f_3 moved in ahead of p_2, almost touching it. A tight filament twisted in between them, and the field gradient was very large indeed. Although f_3 did not take obvious part in the flares, its motion to west was every bit as remarkable as that of f_1--in fact on August 6 the filament passes around f_3 and it is an island of *f* polarity inside the *p* penumbra. Although the group gave the appearance of an extremely active one, there was in fact little activity aside from the great flares. Most of the smaller flares were two strand or two-point flares which may be used to determine the ends of flux loops, for example one at 01:02 August 5 connected p_1 and f_3 and several flares connecting p_3 and f_1.

Probably the most important consequence of the August flare was the rapid separation of p_3 from p_2. As can be seen in the off-band pictures of Figure 4, p_3 appeared separate from p_2 at dawn on the 3rd and steadily drew apart, producing a winding in the neutral line between f_1 and p_3. There was also a rapid motion of f_2 towards f_1 after August 4. This motion occurred in the opposite direction to the movement of p_3. It is likely that both motions worked to increase the shear of the filament between them. These spot motions were generally very slow with a mean velocity 30 m/sec - 50 m/sec.

But they occurred steadily and in two or three days there were always noticeable changes in spot configurations as well as large increases of shear in the neutral line. Obviously such changes were necessary for a big flare to occur as the observed intervals between big flares show.

There were no more flares with footpoints in p_2. There was considerable small surge activity in the area just following p_3 on the *f* side of the neutral line. Such activity is characteristic of emerging flux, and the magnetograms for August 4, 5, and 6, in fact, show *p* polarity which was part of the emerging dipole imbedded in the *f* polarity region (Figure 6). Dark fibrils connected this flux to f_1. Eventually on August 7, the *p* flux broke through and filled this region. Small flares at 01:37 and 16:53 on August 5 extended along the dark fibrils from the EFR to f_1 and p_3, while the flare at 01:00 had just two bright points at p_1 and f_3. There was also rapid growth of new *p* spots following p_1 and just across the neutral line from f_1.

On the 6th, the dark filament, *fil 1*, now stretched all the way through the region and around to the *p* side. It was, of course, no ordinary filament, but a complex of twisted dark fibrils along the neutral line. Spot p_3 shrank and there were penumbral fibrils parallel to the neutral line (east-west). Large velocity shear was observed in this penumbra on August 7. During the 6th, dark loops were visible on the red wing of Hα, pouring down into f_1.

VIII. THE GREAT FLARE OF AUGUST 7

Observations at Tel Aviv showed high plage brightness in the early hours of the 7th; when observations began at Big Bear at 13:50, there was a flare in progress following f_1. OSO-7 shows a steady increase in soft x-rays beginning at 10:00. The filament winding E of p_3 was continually active, and a small flare encircled p_3 at 14:42. Hα spectrum scans taken at 14:50 showed very wide and slightly tilted absorption features at A (Figure 16) with a Doppler width of 80 km/sec, indicating filament activation. A wavelength scan at 15:00 shows strong λ shifts. The cancellation picture (Figure 16) between +0.5 Å and -0.5 Å shows that the activated filament started rising at point A (bright in the figure), and that the other parts of the filament were mostly falling. Note that narrow rising threads were seen in contact with the falling filaments indicating a rolling motion of the filament. At 15:03 the dark feature in the blue wing was moving along the filament from A to B. This was followed immediately by the beginning of the flare at 15:05. The BBSO observations are simultaneously at ± 0.5 Å with 7 sec interval between frames. The first bright points appeared simultaneously over the f_1 umbra, directly across the neutral line in the new spots following p_1, along *fil 1* N of f_1, and just preceding p_3. At 15:12 a bright streak flowed N (down) from spot f_1 along *fil 1* into the northernmost bright element; at the same time the bright *p* points connected. This phase is seen in

Figure 16

Picture showing the cancellation between +0.5 Å and -0.5 Å of Hα at 15:00 on August 1. Bright is rising, dark is falling for the filaments. The position of the spots is shown by broken lines. At the rising part (A) of the filament, the absorption spectrum with 1.8 Å wide (Doppler width) was observed at 14:52.

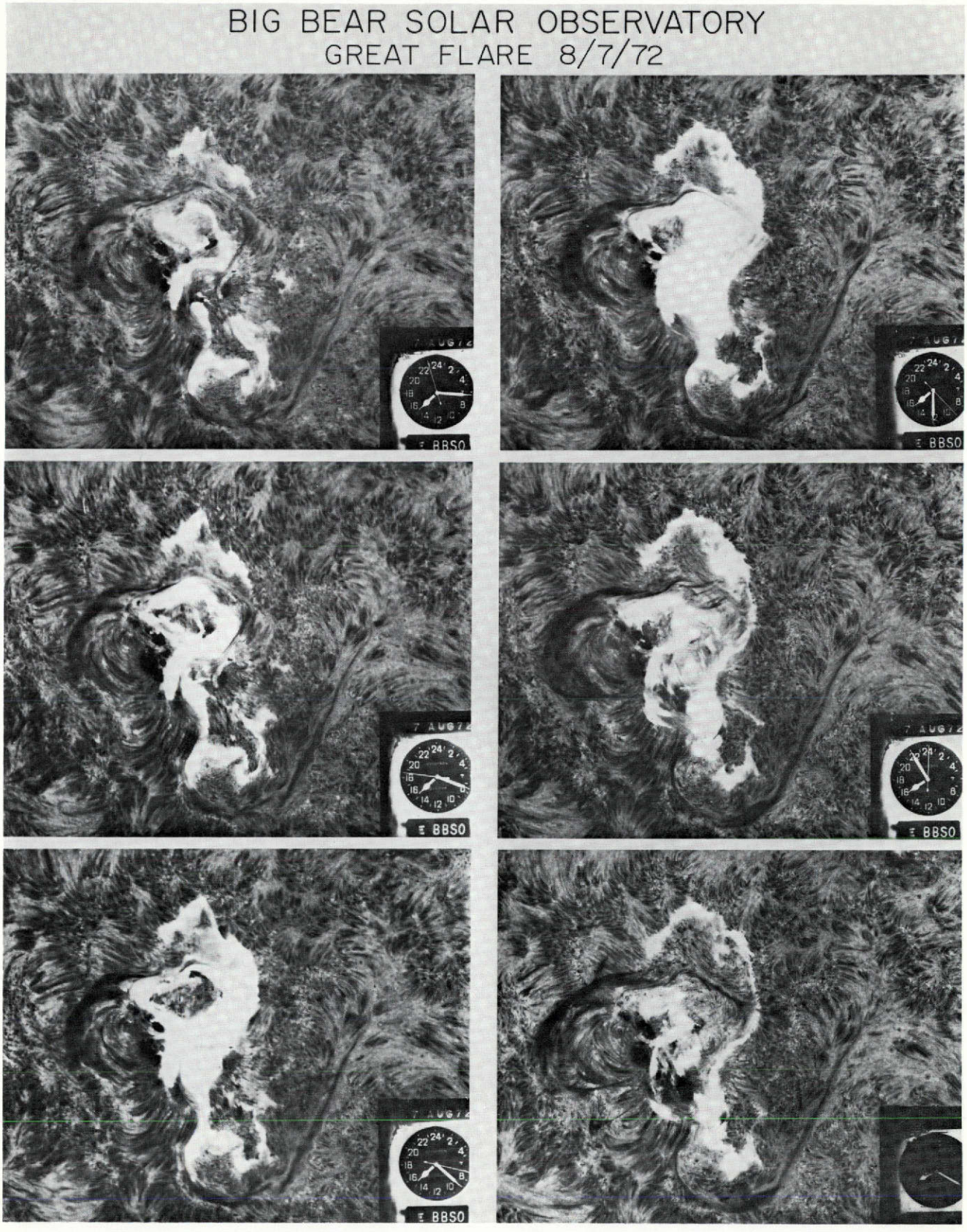

Figure 17

Development of the August 7 flare, Hα - 1/2 Å. The intense kernels are located in f_1 and the lower half of the area curling just above the neutral line. Note the bright strands in the late phase of the flare.

the first frame of Figure 17. Now the main growth took place in the *p* region, first (15:15) preceding p_3, then (15:18) on the arc from p_1 to p_3. This brightening flowed along to p_2, then bounced back at 15:21:00, and when it hit the neutral line at 15:22 there was an enormous brightening all over, particularly in the *p* polarity, including, for the first time, the *f* polarity area directly across from p_3. This was the peak of the flash phase and appears to agree with the peak of the radio burst. However, spectra and dark prints show that the newly brightened area was much fainter than the two flare kernels. The flare continued to grow, albeit more slowly, particularly spreading over all the *p* spots except p_1 and forming an elegant sea-horse shape. On the 37 GHz records from Slough there are peaks at 15:16, 15:18, and 15:21.5, which appear to correspond to the stages enumerated above; this confirms our feeling that "quasi-periodic" microwave and x-ray pulsations, noted by Frost (1969) are just successive energy releases in different areas, the time spacing being the time it takes an MHD wave to cross the region. Where such velocities are seen as the advance of distinct bright fronts, we measure about 600 km/sec. However, if we look at the flare on a dark print (Figure 18), we find that only two areas over f_1 and the curved branch on the *p* side are very bright--the rest of the Hα flare is much weaker and only appears as bright because of the saturation of the print. Note that *fil 1* was completely disrupted in the flare region but relatively unaffected outside. At 15:28 the first bright loops (obviously corresponding to

the loop prominences one might see at the limb) appeared crossing in the center of the flare, almost parallel to the neutral line (Figure 18). With the disappearance of these loops, new loops (dark in later phases) successively appeared, making greater angles to the neutral line. Figure 19 shows time variation of the tilt of the loops to the neutral line at various places in the center of the flare; it increased rapidly until 15:40, and continued to increase slowly in the late phase of the flare. Similar changes in the loops were also observed in the August 4 flare showing the same time history as this flare (indicated by a line in Figure 19). Loops were connected at foot points to the two emission ribbons, which moved steadily outward with a velocity of 2 km/sec.

Apparently the loops formed later higher than those formed earlier. We could actually see in later phases of the limb flare of August 11 that semi-circular loops appeared successively at higher places with the apparent rising velocity of 1.7 km/sec, which was about equal to the separation velocity of the two ribbons of the August 7 flare. We conclude from this change of tilts that the field at the surface runs along the neutral line, while at greater heights the field lines run at successively greater angles to the neutral line, getting closer to a potential field which connects p and f polarity with the minimum energy. This sheared structure of fields may have existed from the start; as the flare plasma cools, condensation takes place in successively higher loops. Alternatively, higher loops with less energy may represent

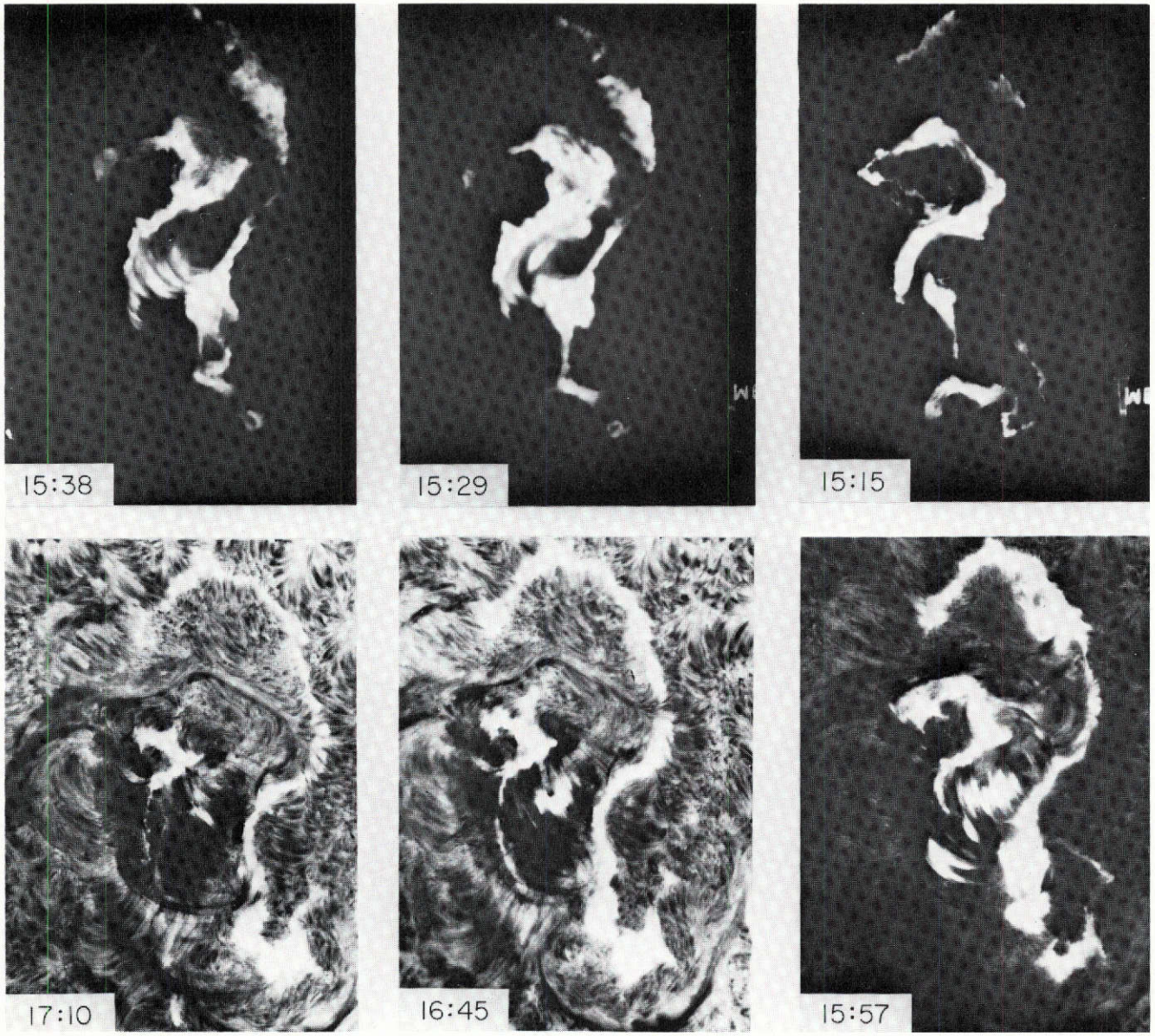

Figure 18

Dark prints showing the development of the flare loops in the August 7 flare, Hα + 1/2 Å. The first loop appeared at 15:29, crossing the neutral line at a sharp angle. The loops are dark in the last two pictures except the center.

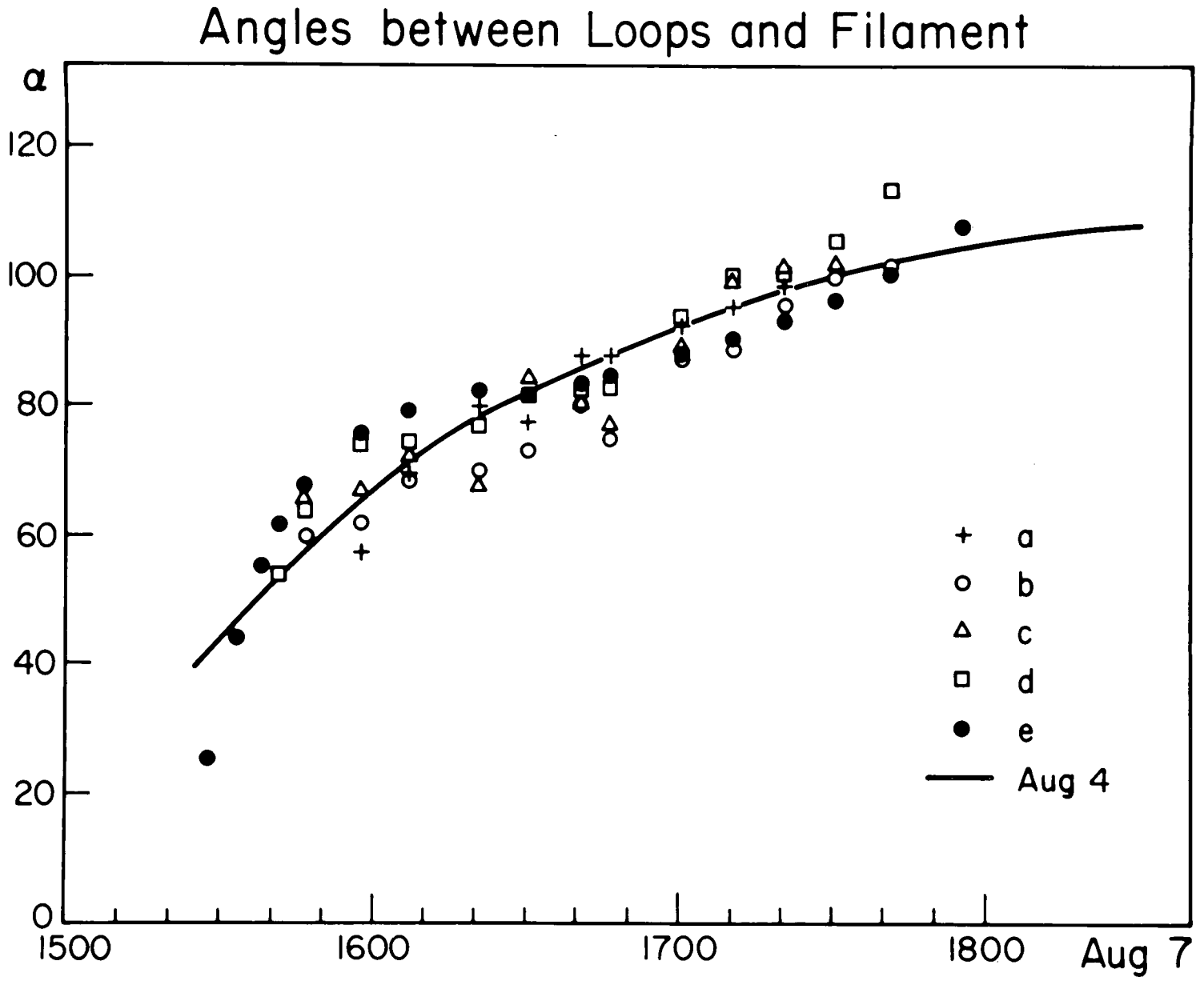

Figure 19

Time variations of the angles between the loops and the filament (the neutral line) at the center portion of the August 7 flare. The line shows the similar variation in the August 4 flare. (The time is shifted to match the August 7 case.)

re-establishment of potential type field lines after reconnection of low loops, the difference in energy between them being released by some unknown mechanism. This case corresponds to the continuous energy releasein the late phase although the release rate slows down much. In any event, we can say that much of the flare energy is due to successive stripping away of long, highly sheared low field lines, and their replacement by potential fields.

Two emission ribbons moving apart were visible for a long time in all the large flares. In later phases on August 7 we could see dark mottles or spicules appeared crossing above the emission ribbons. Hα emission in these ribbons must originate low in the chromosphere. We have a flare model in which the hot thermal plasma continuously diffuses outward, but the inner part cools faster, because of its greater density and the short distance to the surface, and the hottest plasma is located at the outer edge. In this model loops appear after the gas has cooled to a temperature at which Hα may be emitted. This implies that the outer shell is denser than the inner after it cools; observations of continuum in limb loops have showed a peak density at the height of the loop tops.

IX. SPECTRA OF THE AUGUST 7 FLARE

James Dominy was observing with the Coudé spectrograph, and spectra were taken beginning at 15:00 at 10 sec intervals in Hα. Until 15:16 spectra were taken of the bright area N (below) f_1; at 15:16 the spectrograph slit was shifted to the main bright *p* kernel and its development followed. Slit-jaw Hα pictures show the exact placement of the slit on the flare. The spectra (Figure 20) have been measured on the microdensitometer. Also we planimetered the line profiles and subtracted the background at that point (which was in the penumbra) to get the net flux of Hα emission, which was normalized to the undisturbed continuum away from the spots and the equivalent width plotted in Figure 21. There were two intense kernels of emission in *p* area, which showed maximum line width 12 Å (FWHM) for a few minutes around 15:20 (Figure 20). Also peak intensities up to three times the local continuum level were observed. Profiles at this stage showed red asymmetry of 3 to 10%, centered on 2 Å red, but the peak emission still was at line center. This shift corresponds to the velocity imparted to protons by collisions with electrons moving near the speed of light and may be due to atoms excited or accelerated by collisions with downward moving fast electrons. There is a basic asymmetry in the geometry; if electrons are accelerated above the surface, as they must indeed be, then they can only collide with much material when they move downward, hence a red asymetry must result. Hα fluxes of kernels started to

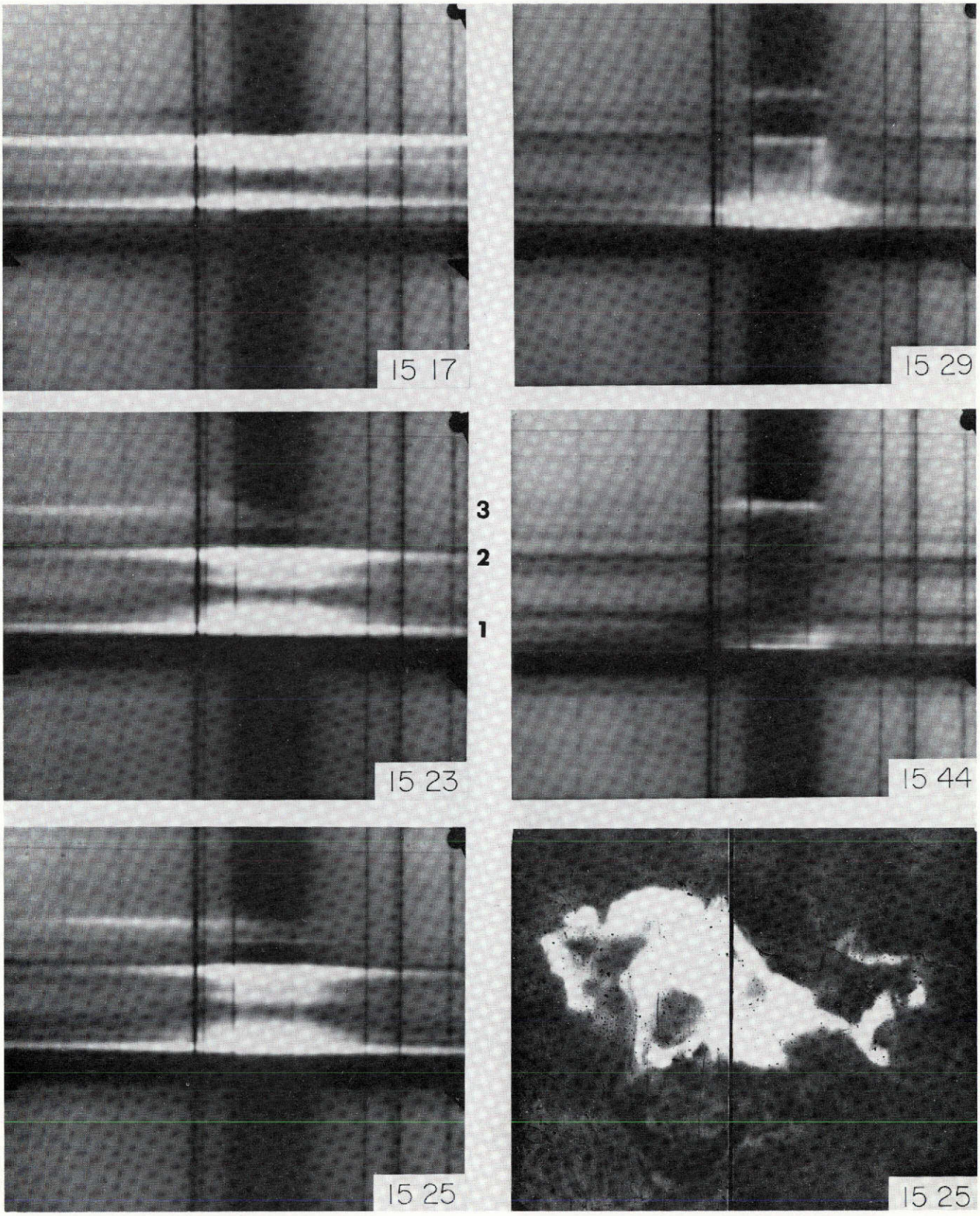

Figure 20

Sequence of Hα spectra taken at the flash phase and the later phase of the August 7 flare. The spectrum covers 10 Å. Dispersion 0.56 Å/mm. Red is to the left. The slit jaw Hα picture at the lower right shows the slit orientation. Note the strongly red-shifted emission (3) at 15:23 and 15:25. Only the kernels (1) and (2) are really broad.

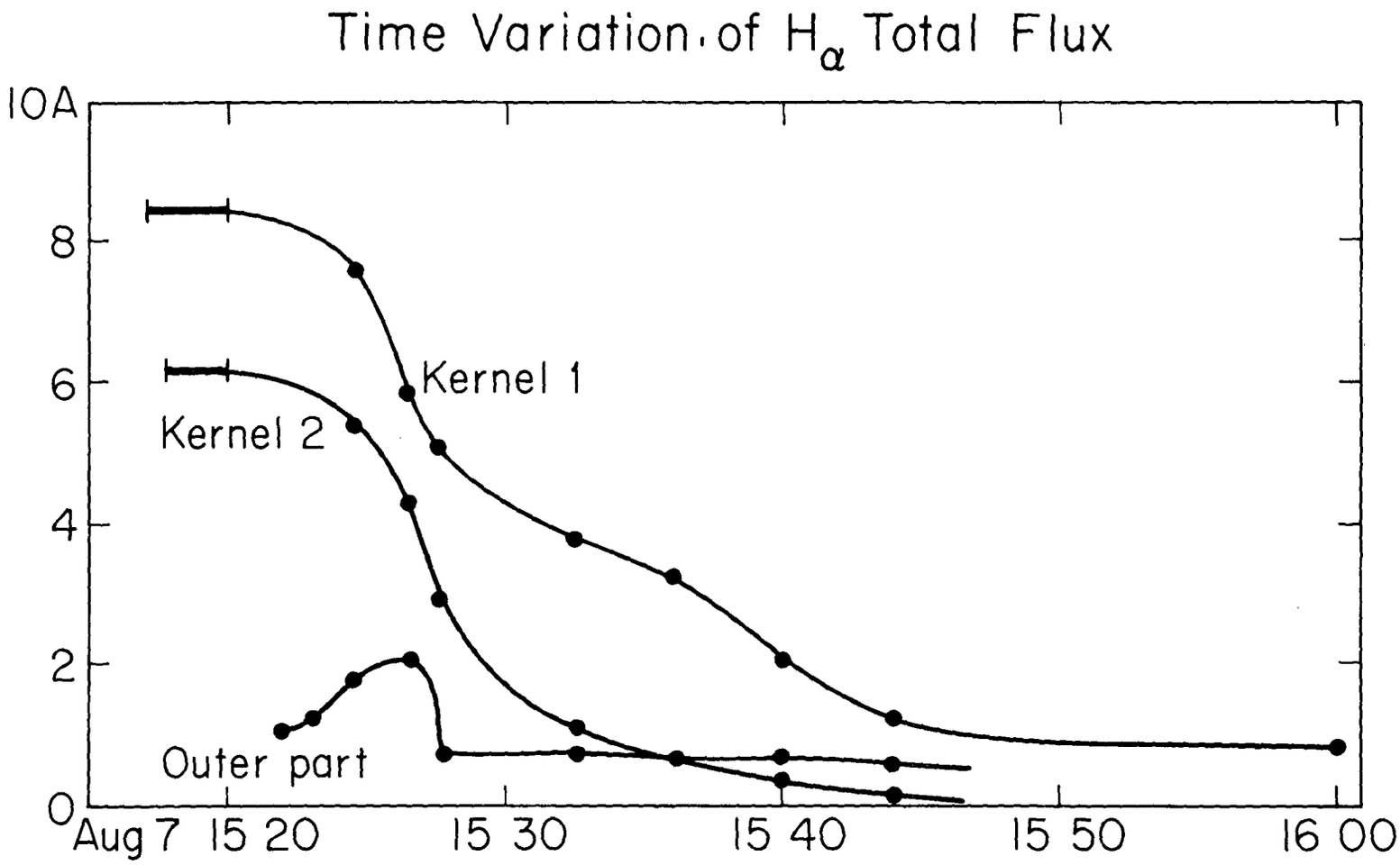

Figure 21

Time variation of Hα total fluxes denoting the net energy between the emission profile and the absorption profile at the quiet time. The energy is shown in wavelength units, referring to the continuum of the quiet region. See Figure 20 for three measured places. (The "outer part" is point (3).) Note that maximum for the flare area was attained at 15:28 after the widest emission disappeared.

decrease from 15:25, but the area of emission was still increasing, showing peaks at 15:28. Thus the total flux of Hα emission stayed rather constant from 15:20 to 15:28.

When emission spread rapidly from p_2 to all the *p* and *f* area at 15:22, strong red shifted emission was observed at the outer part (*f*) of the filament (Figure 20, 15:23). Filtergrams showed much more intense emissions in the red wing than in the blue wing over the whole *f* area and part of the *p* area. Emission appeared 2 Å to the red with a Gaussian profile with an equivalent Doppler width of 2.9 Å. This lasted for 5 minutes and faded after 15:27. This red shift cannot be due to the projection effect of horizontal motion, for the direction of the spread of emission is largely toward us. Thus it must be due to downward moving atoms or downward moving exciters. It should be noted that a dark red shifted feature was seen for ten minutes before emission occurred at the same place (Figure 20 at 15:17). The total energy of the red shifted emission is estimated as equal to 6×10^{28} ergs, which is only a small fraction of the energy of non-thermal electrons. In kernel 1, the blue side of the emission was enhanced after 15:36, and the peak was seen at 0.6 Å blue from 15:40 on (Figure 20). At the same time, kernel 2 showed doubly peaked emission (Figure 20), the peak occurring at 0.5 Å on both wings. This doubly peaked profile is characteristic of flare emission right above the sunspot umbra. The blue asymmetry can be attributed to excess absorption in the red wing since the continuum was depressed in the far red wing. After the rapid

spread of the flare the red-shifted emission was replaced by relatively narrow emission symmetric about the line center.

We must emphasize that all the emission, shifted or unshifted, occurring outside the kernels was relatively narrow and weak compared to the great emission from the flare kernel itself. We can conclude that the main energetic flare occurs in the kernels, and the outer areas are "lit up" as the flare energy spreads to higher flux loops and hot red-shifted material rains down on the surface. The small red asymmetry in the kernel may be due to superposition of the downward falling bright material which covers the flare area or precipitating particles.

The Hα width dropped below 1 Å after 15:45 even in the strongest kernel.

Late in the flare, spectra were obtained in various spectral regions, scanning over the whole flare area. They show a remarkable velocity discontinuity along the neutral line between f_1, f_2 and p_3 in a region which shows penumbra but no sunspot (Figure 22, *x* on the slit). The shear is seen in the spectrum to occur in all spectrum lines, it amounts to 4 to 5 km/sec to the red side, irrespective of line strength, or over 6 km/sec if the motion is in the surface plane of the sun. The motion was seen in spectra up to 19:00, whereupon it stopped.

Off-band pictures before and after the flare show a large change in the direction of the penumbral filaments in this area (just above the *x* on the slit in Figure 22); at 15:00 U.T.

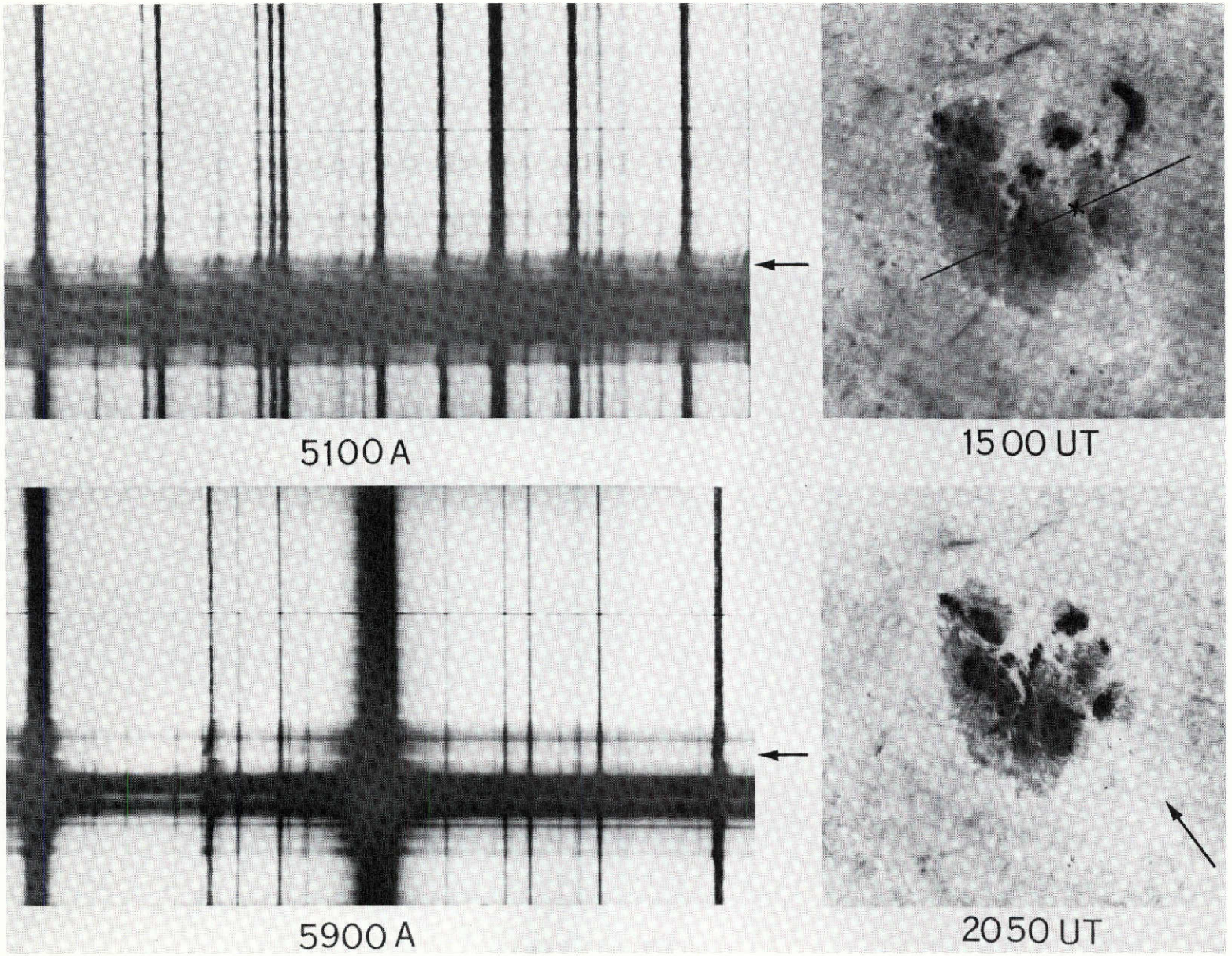

Figure 22

The velocity shear observed during the flare of August 7 (arrow) in spectra taken at 5100 Å and 5900 Å. The off-band picture at 15:00 shows the slit orientation and the place of the velocity shear (point x). The velocity shift is to the red (4 - 5 km/sec) and appears for all the lines. Note that the direction of the penumbral filaments at point x changed after the flare (20:50) as if the flow occurred along the boundary of the penumbra (p_3) towards the arrow shown in the lower right.

these filaments were directed to the northwest or to the direction of the slit in Figure 22, while at 20:50 U.T. their direction changed to the southwest, producing a kink between these penumbral filaments and those in f_1. This change can be explained by the sheared flow in the surface plane seen in the spectra, which dragged the penumbral filaments to the southwest direction. We only measure radial velocity, so the direction of motion may only be deduced from observed changes in penumbral fibrils and the neutral line. The direction of this motion (perpendicular to the neutral line) is such as to increase the shear of the magnetic field lines, as though the photospheric flow is inexorably pushing on either side or it, finally to be released by the flare. There was actually an increase in the shear observed in this part of the fibril from August 6 to the time of the flare. Note that this flow was perpendicular to the motion of spot f_2 towards f_1 which was along the neutral line. The activation of the filament along a segment before the flare is shown in Figure 16 to occur at the southeast edge (A), along a segment anchored in the moving penumbra (also see dark feature at 15:00 U.T. in Figure 22).

Study of before-after pairs shows some change in the spot group after the flare. The east penumbras of f_1 and f_2 shrank appreciably, and p_2 and p_3 umbras shrank rapidly. A few small spots under the *p* kernel changed, but such spots are always changing. There was continued motion of spot f_2 toward f_1, which it joined on the 10th. (The largest motion 0.42 km/sec was found during the flare from 15:00 U.T. to 18:00 U.T.) The

magnetograms show a decrease in the *f* polarity in the area it vacates, and a general southeast expansion of the *p* polarity around p_3. The large filament S-W of the *p* spots, which was active all day on the 7th on the blue wing, disappeared. Further evolution of the group to its limb passage is shown in Figure 5. It gradually simplified and was uninteresting except for the limb flare of the 11th.

X. Hα FLUX

There has been much attention paid to the total Hα flux from great flares in comparison with the total energy. In this case, with continuous Hα spectra and filtergrams on both wings of Hα, we can measure this in a more definitive way. We planimetered dark prints (Figure 18) showing two intense kernels at 15:20, 15:27 and 16:00 U.T. (the end of Hα spectra). At 15:20 U.T., the area of the kernels was $6.0 \times 10^{18} cm^2$ with band width 9.2 eq. Å (equivalent engstroms referred to the continuum). At 15:27, the area of the kernels had increased to $8.5 \times 10^{18} cm^2$ with 6.2 eq. Å width, and at 16:00 it decreased to $1.4 \times 10^{18} cm^2$ with 1.8 eq. Å width. Time histories of the integrated Hα fluxes are shown in Figure 21 for three places. The total flare area in Hα centerline was 4.3×10^{19}, but the line width over most of the area was only about 1 eq. Å in the regions outside the kernel. The contribution from these fainter regions to the total energy was 18%, 28% and 87% at three times mentioned. Applying a filling factor 0.74 for the fraction of the kernel that gives the broad emission on the spectrograms (see Figure 20) and correcting for projection, we find a total Hα emission of 1.2×10^{27}erg/sec at the peak. Integrating over the flare lifetime from 15:10 to 16:10, with an allowance for the later tail-off, we find a total Hα energy in this huge flare of 2.5×10^{30}ergs. Why is this number so much smaller than previously published figures? Because the previous calculations assumed that the broad emission was characteristic of the entire flare area during its entire lifetime. In this case,

comprehensive data enables us to make a much better estimate, accurate within a factor 2. We have no spectra for the August 4 event, but we planimetered it and, assuming the same spectrum as August 7, obtained 2 x 10^{30}ergs, roughly the same as August 7.

If we compare this value with the total proton energy estimated by Ramaty (private communication) as 10^{35} protons above 10 Mev or about 2 x 10^{30}ergs, we see that the Hα energy is comparable to the protons and the hard electrons.

If we consider that energetic phenomena are limited to the kernel from which most of the emission takes place, we may estimate the volume involved by considering it as a loop connecting the two branches of the kernel. Each branch has an area about 1.7 x $10^{18}cm^2$ and the separation is 25000 km, hence for a semicircular loop we get 2 x $10^{27}cm^3$. If the emission measure was $10^{48.3}$ for x-rays above 10 KeV (same as August 4 flare), we get $N_e N_i$ equal 10^{21}, or 3 x 10^{10} hard electrons/cm^3 above 10 KeV! It appears that in this huge event all particles in the kernel are accelerated.

Finally, the dominance of Hα emission from the flare kernel explains the discrepancy usually found between the reported time of "Hα maximum" which refers to the maximum area, and x-ray and radio bursts. A plot of the total Hα energy from the August 7 flare peaked around 15:22, the time of the peaks of radio and x-ray emission, and remained constant up to 15:28. The same time would be derived from peak kernel brightness and peak Hα line width. It would be a considerable improvement if such data could be observed and reported.

XI. CONCLUSIONS

(1) The region exhibited twisted magnetic flux and high gradients from its birth.

(2) The flare occurred because of large shear of the neutral line and high field gradients.

(3) The motions and growths of sunspots occurred producing the invasion of *f* spot to *p* area and increasing the shear of the neutral line.

(4) Development of the post-flare loops revealed sheared structure magnetic field lines above the neutral line; the lowest field runs parallel to the neutral line and the higher field runs more and more perpendicular to it. The flares occur in the transition from the sheared field to the potential field.

(5) The Hα flux of the large flares comes mainly from kernels whose emission peaks with radio and x-rays. The total Hα emission from the great flares of August 4 and August 7 was 2.0×10^{30} and 2.5×10^{30} ergs, respectively.

(6) The Hα emission is 12 Å wide in the flare kernels and only 1 to 2 Å wide in the rest of the flare. This flare halo makes up most of the area and thus determines the assigned "importance" but only produces 1/4 of the Hα emission.

(7) In 3835 band we detected rapidly varying emission at the edges of the flux loops. The emission can be explained by the dumping of the 50 KeV electrons accelerated in individual flux loops.

(8) Comparison of the 3835 flashes with the x-rays and microwave emissions shows that thick foil models of x-ray emission are more consistent than the thin foil model for the impulsive flare.

(9) We observed the large velocity shear of absorption lines in the flare region. This explains the rapid change of the fibril orientation observed in the penumbra which may be related to the cause of the flare.

ACKNOWLEDGEMENTS

We are indebted to many colleagues who supplied their data for this study, in particular to Dr. Dayton Datlowe, UCSD, and Dr. John Castelli, AFCRL, and James Mosher. We thank also Drs. H. Hudson and S. Enome for discussions. The Big Bear observations were made by James Mosher, Tom Pope, David Glackin, James Dominy, David Brin, John Morgan, Douglas Rabin and the authors. A 16 mm film of the flares is available at cost ($30.00).

This work has been supported by NASA under NGR 05 002 034, NSF Atmospheric Sciences program under GA 24015, and AFCRL under FI9628-73-C-0085.

REFERENCES

Brown, J.: 1972, Solar Phys. 26, 441.

Fermi, E.: 1949, Nuclear Physics P., The University of Chicago Press.

Frost, K.J.: 1969, Ap. J. 158, L159.

Hudson, H.S.: 1972, Solar Phys. 24, 414.

Lincoln, J.V. and Leighton, H.: 1972, Report UAG-21, World Data Center A, p. 80.

Ramaty, R. and Petrosian, V.: 1972, Ap. J. 178, 241.

Schatzman, E.: 1965, The Solar Spectrum, de Jager ed., P313, D. Reidel Publishing Company, Dordrecht-Holland.

Syrovatskii, S.I. and Shmeleva, O.P.: 1972, S.A.J. 16, 273.

Takakura, T.: 1967, Solar Phys. 1, 304.

Tanaka, K., and Zirin H.: 1973, The Symposium on High Energy Phenomena on the Sun, in press, Ramaty ed.

Uchida, Y.: 1972, pre-print.

Zirin, H.: 1972, Solar Phys. 22, 34.

Zirin, H., Pruss, G. and Vorphal, J.: 1971, Solar Phys. 19, 463.